SIAM J. APPL. MATH.
Vol. 81, No. 3, pp. 1166–1189

IMPACT OF VARYING COMMUNITY NETWORKS ON DISEASE INVASION*

STEPHEN KIRKLAND†, ZHISHENG SHUAI‡, P. VAN DEN DRIESSCHE§, AND XUEYING WANG¶

Abstract. We consider the spread of an infectious disease in a heterogeneous environment modeled as a network of patches. We focus on the invasibility of the disease, as quantified by the corresponding value of an approximation to the network basic reproduction number, $\mathcal{R}_0$, and study how changes in the network structure affect the value of $\mathcal{R}_0$. We provide a detailed analysis for two model networks, a star and a path, and discuss the changes to the corresponding network structure that yield the largest decrease in $\mathcal{R}_0$. We develop both combinatorial and matrix analytic techniques, and we illustrate our theoretical results by simulations with the exact $\mathcal{R}_0$.

Key words. basic reproduction number, matrix-tree theorem, group inverse

AMS subject classifications. 92D30, 92D25, 15A09, 15A18

DOI. 10.1137/20M1328762

1. Introduction.

Advanced science and technology have made our world an increasingly connected place. Globalization and urbanization bring not only benefits but also attendant consequences such as the spread of emerging and re-emerging infectious diseases. Historically, plague, cholera, and influenza have resulted in millions of human deaths, and insight into the spread and control of these diseases has shaped our modern society, particularly in medicine and public health. Recent emerging diseases such as HIV/AIDS, SARS, Ebola, and COVID-19 highlight the need for scientific investigations of disease spread via transport networks [43]. As disease vectors (e.g., mosquitoes and ticks) can also be carried via human/goods transport, the outbreak and spread of vector-borne diseases such as dengue, Lyme disease, malaria, West Nile virus, yellow fever, and Zika virus have exhibited strong spatio-temporal patterns [15, 22, 26, 37, 40, 41, 42, 47] (also see the recent special issues [31, 39]); this is partly due to the interplay between disease epidemiology and vector ecology. Spatio-temporal patterns have also been observed for many waterborne diseases caused by pathogenic micro-organisms such as bacteria and protozoa that are transmitted in water/river networks [3, 20, 33, 38, 45, 46]. One of the main scientific challenges is to determine the connection between disease risk and the change of network structures (as a consequence of human behavior and/or environmental uncertainty). Recent studies using statistical data from climate, environmental, and disease surveillance have shown in-

*Received by the editors April 1, 2020; accepted for publication (in revised form) March 1, 2021; published electronically June 10, 2021.
https://doi.org/10.1137/20M1328762
Funding: The first author was partially supported by NSERC Discovery grant RGPIN–2019–05408. The second author was partially supported by NSF grant DMS-1716445. The third author was partially supported by NSERC Discovery grant RGPIN–3677–2016. The fourth author was partially supported by Simons Foundation grant 317407.
†Department of Mathematics, University of Manitoba, Winnipeg, MB, R3T 2N2, Canada (Stephen.Kirkland@umanitoba.ca).
‡Department of Mathematics, University of Central Florida, Orlando, FL 32816 USA (shuai@ucf.edu).
§Department of Mathematics and Statistics, University of Victoria, Victoria, BC, V8W 2Y2, Canada (pvdd@math.uvic.ca).
¶Department of Mathematics and Statistics, Washington State University, Pullman, WA 99164-3113 USA (xueying@math.wsu.edu).

consistent and geographically variable results. For example, a discrepancy in the correlation with precipitation has appeared in the literature of waterborne diseases: a significant positive association between heavy rainfall and waterborne diseases is often observed [9, 13, 16, 23, 32] (also see the review paper [30]), while increased prevalence of waterborne diseases has also been reported as an unexpected consequence of drought [6] and the anthropogenic protection against annual flooding [10]. Although detailed discussions of this discrepancy, as a consequence of human behavior and/or climate change, have been surveyed in [4, 29], rigorous scientific explanations and theoretical insights are lacking, due to the complexity and multiple time scales.

Many existing studies in the literature have focused on the aggregation of disease dynamics at each geographical region (or patch) via a static movement (or community) network and emphasized either the situation where the time scale of the dispersal among patches is much faster than the scale of patch demography/disease dynamics, or with the focus on the monotonicity of disease invasibility with respect to dispersal speed or travel frequency; see, for example, [1, 8, 17, 18, 19, 44]. Recently, a general result on the spectral monotonicity of a perturbed Laplacian matrix in [12] has provided theoretical insight on the aggregation. Specifically, for a square matrix $A = Q - \mu L$, where $Q = \mathrm{diag}\{q_k\}$ is a diagonal matrix encoding within-vertex (within-patch) population/disease dynamics, and L is a Laplacian matrix describing population dispersal among patches in a heterogeneous environment (of n patches), the monotonicity and convexity of the spectral abscissa of A, $s(A)$, with respect to dispersal speed μ, are established: $\frac{ds(A)}{d\mu} \leq 0$ and $\frac{d^2 s(A)}{d\mu^2} \geq 0$. The limiting behavior with a faster time scale of population/disease dynamics is similar to the decoupled (no movement) system, $s(A) = \max\{q_k\}$, while the limiting behavior with a faster time scale of dispersal is the u-weighted average, $s(A) = \sum_{k=1}^{n} u_k q_k$, where $u = (u_1, u_2, \ldots, u_n)^\top$ is the normalized right null vector of L. As pointed out in [12], these results also are related to the reduction principle in evolutionary biology [2, 25] and the evolution of dispersal in patchy landscapes [27]. For many heterogeneous infectious disease models, the network basic reproduction number $\mathcal{R}_0$, a threshold determining whether the disease dies out or persists, can be approximated as the u-weighted average of the individual patch reproduction numbers $\mathcal{R}_0^{(k)}$, $\mathcal{R}_0 = \sum_{k=1}^{n} u_k \mathcal{R}_0^{(k)}$, when the dispersal among geographic regions is faster than the disease/population dynamics; see, e.g., [17, 44] for waterborne diseases, [12, 19, 21] for general diseases of susceptible-infectious-susceptible (SIS) or susceptible-infectious-recovered (SIR) type, and [8] for the analogue in a continuous spatial landscape.

In this paper, we investigate the impact of varying community networks on disease invasion in a heterogeneous environment. Our motivation comes from the spread of a waterborne disease, such as cholera, in a heterogeneous network [17, 44], in which the pathogen (the bacterium *Vibrio cholerae*) travels within a hydrological landscape (e.g., a river network) or the spread of directly transmitted diseases for which the host moves between regions [1]. If the network structure changes, our goal is to determine how this affects the network basic reproduction number $\mathcal{R}_0$ for the spatial spread of the disease. The quantity $\mathcal{R}_0$ is important as it usually determines a threshold for disease extinction (when $\mathcal{R}_0 < 1$) or persistence (when $\mathcal{R}_0 > 1$) and gives guidance for disease control strategies.

First, we consider a toy model of a 4-node path graph network with counterintuitive numerical results showing opposite monotonicity of $\mathcal{R}_0$ corresponding to a bypass from upstream to downstream (e.g., due to flooding). For the reader's convenience, in supplementary material section (A) we include the model and re-

lated results from [17, 44]. As depicted in Figure 1, we consider the spread of a pathogen (e.g., cholera) on a path network of 4 patches (vertices) with vertices 1, 2, 3, 4 sequentially located along a river, where vertex 1 is upstream and vertex 4 is downstream. We assume that each nonzero movement rate, m_{ij} from vertex j to vertex i, on the path has value 1. As shown in [17, 44] the associated next generation matrix takes the form $K = FV^{-1} = D_q G_W^{-1} D_r G_I^{-1}$, where F is the matrix of new infections, V is the matrix of transitions, $D_q = \mathrm{diag}\{q_i\}$, $G_W = \mathrm{diag}\{\delta_i\} + L$, $D_r = \mathrm{diag}\{r_i\}$, and $G_I = \mathrm{diag}\{\mu_i\}$. Here the parameters q_i, δ_i, r_i, and μ_i are the linearized indirect transmission rate (from pathogen to host), pathogen decay rate, pathogen shedding rate, and decay rate of infectious host individuals in patch i, respectively ($i = 1, 2, 3, 4$). The matrix L is the 4×4 Laplacian matrix associated with M, i.e., $L = \mathrm{diag}\{\sum_{j \neq i} m_{ji}\} - M$, where $M = (m_{ij})$ with $m_{ij} \geq 0$ representing the pathogen/host dispersal from patch j to patch i. Then the exact network basic reproduction number is $\mathcal{R}_0 = \rho(FV^{-1}) = \rho(D_q G_W^{-1} D_r G_I^{-1})$, where ρ denotes the spectral radius. For simplicity, we set $r_i/\mu_i = 1, \delta_i = 1$ in each patch, with the base q_i value taken to be $q = 0.195$. In this case, the basic reproduction number in patch i is equal to q_i. We consider two scenarios in which the network has a "hot spot," i.e., a vertex i at which the linearized indirect transmission rate q_i (or, equivalently, $\mathcal{R}_0^{(i)}$) is higher than those of the other vertices, and an arc that bypasses the hot spot. In the first case (see the left plot in Figure 1), the hot spot is assumed to be located at vertex 2, with an additional bypass downstream from vertex 1 to vertex 3 included, specifically, $q_1 = q_3 = q_4 = q$, $q_2 = 10q$, and

$$L = \begin{pmatrix} 1 + m_{31} & -1 & 0 & 0 \\ -1 & 2 & -1 & 0 \\ -m_{31} & -1 & 2 & -1 \\ 0 & 0 & -1 & 1 \end{pmatrix}.$$

In the second case (see the right plot in Figure 1), the hot spot is located at vertex 3, and a new bypass from vertex 2 to vertex 4 is included with $q_1 = q_2 = q_4 = q$, $q_3 = 10q$, and

$$L = \begin{pmatrix} 1 & -1 & 0 & 0 \\ -1 & 2 + m_{42} & -1 & 0 \\ 0 & -1 & 2 & -1 \\ 0 & -m_{42} & -1 & 1 \end{pmatrix}.$$

In both cases the hot spot is bypassed, in the same direction, but the effects on $\mathcal{R}_0$ are markedly different, as shown in Figure 1. Although symmetric movement is used in the simulations for Figure 1, the inclusion of a small amount of advection (i.e., changing the subdiagonal entries to a common value slightly less than -1 to reflect the upstream-downstream movement) gives the same monotone properties of $\mathcal{R}_0$. Similar behavior also occurs in the simulations of other patch disease models, such as the directly transmitted disease (SIS) model in [1]; see the supplementary material for $\mathcal{R}_0$. These unexpected behaviors motivate our investigation of the effect of network structure on $\mathcal{R}_0$.

The remainder of the article is organized as follows. Some preliminary results are provided in section 2. Two different methods, one combinatorial and the other algebraic, are employed to investigate the impact of varying community networks on disease invasion (sections 3 and 4, respectively). Applications to specific networks are illustrated in section 5 and include an explanation of the counterintuitive numerical

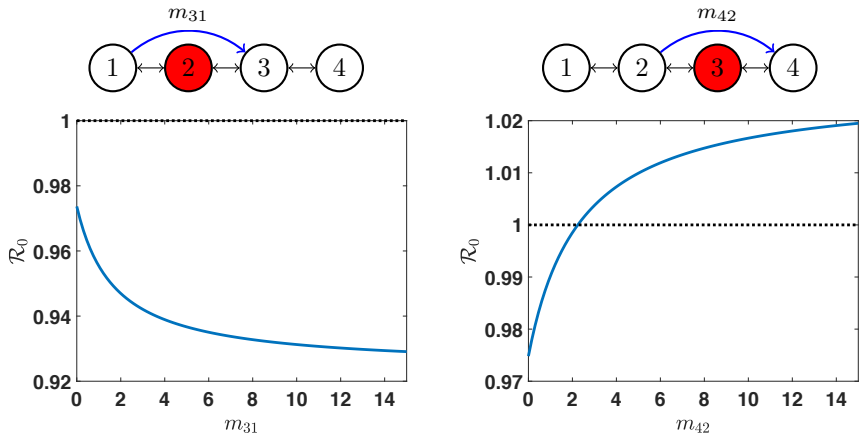

FIG. 1. *With the hot spot at* 2, $\mathcal{R}_0$ *decreases as* m_{31} *increases (left plot); with the hot spot at* 3, $\mathcal{R}_0$ *increases as* m_{42} *increases (right plot).*

results above. Disease control strategies involving varying the community network are considered in section 6, and concluding remarks are given in section 7.

2. Preliminaries. From consideration of a system of ordinary differential equations governing the dynamics of cholera under the assumptions that humans become infected through contact with pathogens in the contaminated water and that the water movement is faster than the pathogen decay rate, it has been established [17, 44] that $\mathcal{R}_0$ is approximated (from the exact value given by the spectral radius of the next generation matrix) by a linear combination of the basic reproduction numbers in each patch in isolation. The constants in this linear combination are the components of the normalized right eigenvector of the Laplacian matrix of the community network. The specific aim of this work is to determine how this eigenvector and $\mathcal{R}_0$ change with alterations in the network structure. We consider a strongly connected network and assume that the network maintains this property when changed.

More precisely, let $M = (m_{ij}) \geq 0$ denote an $n \times n$ irreducible matrix representing the pathogen/host movement in a heterogeneous environment of n patches. In particular, when $1 \leq i, j \leq n$ are distinct, $m_{ij} \geq 0$ represents the pathogen/host dispersal from patch j to patch i. We assume that $m_{ii} = 0$ for $i = 1, \ldots, n$. Let $\mathcal{G} = \mathcal{G}(M)$ be the weighted digraph associated with M. That is, in $\mathcal{G}$ there is an arc $j \to i$ from vertex j to vertex i of weight m_{ij} if and only if $m_{ij} > 0$. Let L be the Laplacian matrix of $\mathcal{G}(M)$, i.e.,

$$L = \operatorname{diag}\Big(\sum_{i\neq 1} m_{i1}, \sum_{i\neq 2} m_{i2}, \ldots, \sum_{i\neq n} m_{in}\Big) - M. \tag{2.1}$$

Notice that each column sum of L is 0, and thus 0 is an algebraically simple eigenvalue of L (since M is irreducible). Evidently the all ones vector, $\mathbb{1}^\top$, is a left null vector for L. For each $k = 1, \ldots, n$, let $C_{kk} = \det(L_{(k,k)})$ be the principal minor of L formed by deleting its kth row and column. Consider the vector $u = (u_1, u_2, \ldots, u_n)^\top$, where

$$u_k = \frac{C_{kk}}{\sum_{\ell=1}^{n} C_{\ell\ell}}, \qquad k = 1, \ldots, n. \tag{2.2}$$

Denote the adjugate of L by $adj(L)$, and recall that $L\,adj(L) = adj(L)L = \det(L)I = 0$.

Hence $adj(L) = x\mathbb{1}^\top$, where x is a nonzero vector in the right null space of L. It now follows that u is the right null vector of L, normalized so that $\mathbb{1}^\top u = 1$.

As shown in [17, 44] (also see [8]), when the time scale of movement is substantially larger than the time scale of the disease dynamics, the coefficients u_k defined above serve as weights to aggregate the disease dynamics from each patch. For this reason, u_k is called the *network risk* of patch k. In particular, the network basic reproduction number $\mathcal{R}_0$ can be approximated by the u-weighted average of the patch basic reproduction numbers $\mathcal{R}_0^{(k)}$, that is,

$$\mathcal{R}_0 \approx \sum_{k=1}^{n} u_k \mathcal{R}_0^{(k)}. \tag{2.3}$$

This expression (2.3) separates the structure of the movement network and the within-patch disease dynamics and thus provides a new approach to investigating the impact of changes in the network on disease invasion. Specifically, we first investigate how a change to the network structure affects the network risks u_k, and then we utilize the aggregation in (2.3) to understand how varying the network affects disease invasibility (i.e., the value of $\mathcal{R}_0$).

Since u_k depends on the cofactor C_{kk} as in (2.2), it can be expressed in terms of the sum of weights of spanning rooted trees [11, 36] by using Kirchhoff's matrix-tree theorem. Calculating the weights of such trees gives a combinatorial method for finding the sign of $\frac{du_k}{dm_{ij}}$, the derivative of u_k with respect to a change in the arc $j \to i$. This combinatorial approach is developed in section 3 and may be convenient for some cases, such as small networks or networks with specific structures.

In addition, there is a well-established algebraic tool for understanding how changes in the movement matrix M affect the entries in the right null vector u of the Laplacian matrix L. Since L is a singular and irreducible M-matrix, the eigenvalue 0 of L is algebraically simple; so, while L is not invertible, it has a *group inverse*, that is, a unique matrix $L^\#$ such that $LL^\# = L^\#L, LL^\#L = L$, and $L^\#LL^\# = L^\#$. The group inverse has been used effectively to analyze how changes in an irreducible nonnegative matrix affect its Perron eigenvalue and eigenvector (see, for example, [14, 34]), and our results in section 4 are informed by that approach. We refer the interested reader to [7] for background on generalized inverses in general and to [28] for the use of group inverses in the study of M-matrices in particular.

With the group inverse method developed in generality, in section 5.1 we illustrate this method with a star network in which one patch is the hub connected to several leaf vertices. Such a network structure is appropriate as a model for a large city connected to smaller cities or suburbs, with humans commuting in each direction. Then in section 5.2, we illustrate the general results for a path network, which models cholera outbreaks in communities along a river. For these two network structures, we consider control strategies for restricted cases of the two networks (section 6) and derive results on how changes to the network can help to minimize disease invasion.

3. Combinatorial method: Counting spanning rooted trees. It follows from Kirchhoff's matrix-tree theorem [11, 36] that the cofactor of the (k, k) entry of L can be interpreted in terms of spanning rooted trees,

$$C_{kk} = \sum_{\mathcal{T} \in \mathbb{T}_k} w(\mathcal{T}) =: W_k, \tag{3.1}$$

where $\mathbb{T}_k$ is the set of spanning in-trees rooted at vertex k, and $w(\mathcal{T}) = \prod_{(j,i)\in E(T)} m_{ij}$ is the weight of a spanning in-tree $\mathcal{T}$ rooted at k. The notation W_k introduced in

(3.1) is convenient for tracking how $u_k = \frac{W_k}{\sum_\ell W_\ell}$, defined in (2.2), behaves as the network structure changes. Specifically, we consider a small change of the m_{ij} value (for a fixed ordered pair (i,j)) in the movement network, say $m_{ij} \to m_{ij} + \epsilon$, and explore how the value of u_k responds; to do so, we focus on the sign of $\frac{du_k}{dm_{ij}}$. (We note in passing that if m_{ij} is zero, we only consider positive values of ϵ, and in that setting $\frac{du_k}{dm_{ij}}$ is interpreted as the derivative from the right.) Notice that such a change $m_{ij} \to m_{ij} + \epsilon$ affects two entries of L, the (i,j) entry and the (j,j) entry.

Before establishing our main results, we introduce some additional notation and tools from matrix theory and graph theory. Let $L_{(ij,k\ell)}$ denote the matrix obtained from L by deleting the ith and jth rows and kth and ℓth columns. Let W_k^{ij} denote the sum of the weights of all spanning in-trees rooted at k containing the arc $j \to i$, and let $W_k^{\sim ij}$ denote the sum of the weights of all spanning in-trees rooted at k that do not contain the arc $j \to i$. Notice that $W_k = W_k^{ij} + W_k^{\sim ij}$.

First, we prove the following two lemmas.

LEMMA 3.1. *Assume $i \neq j$. Then*

$$W_k^{ij} = m_{ij} |\det(L_{(ij,kj)})|. \tag{3.2}$$

Proof. From the all minors matrix-tree theorem [11], $|\det(L_{(ij,kj)})|$ is the sum of the weights of all spanning forests $\mathcal{F}$ that contain exactly two in-tree components, one rooted at k containing vertex i and the other rooted at j. Adding the arc $j \to i$ of weight m_{ij} in $\mathcal{F}$ yields a spanning in-tree $\mathcal{T}$ rooted at k containing $j \to i$; in particular, $m_{ij} w(\mathcal{F}) = w(\mathcal{T})$. The identity (3.2) follows after performing this operation for all spanning forests. ∎

We note here that strictly speaking, the right side of (3.2) is not defined in the case when $k = j$. However, we may adopt the convention that $\det(L_{(ij,kk)}) = 0$, and then (3.2) will also hold when $k = j$.

LEMMA 3.2. *Let $W_k = C_{kk} = \det(L_{(k,k)})$. Then, for any $i \neq j$,*

$$\frac{dW_k}{dm_{ij}} = |\det(L_{(ij,kj)})|. \tag{3.3}$$

Proof. Straightforward calculations, along with (3.2), yield

$$\begin{aligned}
\frac{dW_k}{dm_{ij}} &= \lim_{\epsilon \to 0} \frac{(W_k^{ij} + W_k^{\sim ij})|_{m_{ij}+\epsilon} - (W_k^{ij} + W_k^{\sim ij})|_{m_{ij}}}{\epsilon} \\
&= \lim_{\epsilon \to 0} \frac{(m_{ij} + \epsilon)|\det(L_{(ij,kj)})| + W_k^{\sim ij} - m_{ij}|\det(L_{(ij,kj)})| - W_k^{\sim ij}}{\epsilon} \\
&= |\det(L_{(ij,kj)})|,
\end{aligned}$$

resulting in (3.3). ∎

As with (3.2), when $k = j$, we interpret both sides of (3.3) as being zero.

In particular, if $m_{ij} > 0$ for $i \neq j$, it follows from Lemmas 3.1 and 3.2 that

$$\frac{dW_k}{dm_{ij}} = \frac{W_k^{ij}}{m_{ij}}. \tag{3.4}$$

Now we are ready to prove the main result arising from this combinatorial method.

THEOREM 3.3. *For any given k, i, j, $i \neq j$,*

$$\operatorname{sgn}\Big(\frac{du_k}{dm_{ij}}\Big) = \operatorname{sgn}\Big(\big|\det(L_{(ij,kj)})\big| \sum_{\ell\neq k} W_\ell - W_k \sum_{\ell\neq k} \big|\det(L_{(ij,\ell j)})\big|\Big). \tag{3.5}$$

If, in addition, $m_{ij} > 0$, then

$$\operatorname{sgn}\Big(\frac{du_k}{dm_{ij}}\Big) = \operatorname{sgn}\Big(W_k^{ij} \sum_{\ell\neq k} W_\ell^{\sim ij} - W_k^{\sim ij} \sum_{\ell\neq k} W_\ell^{ij}\Big). \tag{3.6}$$

Proof. Taking the derivative on both sides of (2.2) with respect to m_{ij} yields

$$\frac{du_k}{dm_{ij}} = \frac{1}{(\sum_\ell W_\ell)^2}\Big(\frac{dW_k}{dm_{ij}} \sum_\ell W_\ell - W_k \sum_\ell \frac{dW_\ell}{dm_{ij}}\Big). \tag{3.7}$$

Substituting (3.3) into (3.7), after the cancellation of the case $\ell = k$, yields (3.5).

Additionally, if $m_{ij} > 0$, then it follows from (3.4) that

$$\frac{du_k}{dm_{ij}} = \frac{1}{(\sum_\ell W_\ell)^2}\Big(\frac{W_k^{ij}}{m_{ij}} \sum_{\ell\neq k} W_\ell - W_k \sum_{\ell\neq k} \frac{W_\ell^{ij}}{m_{ij}}\Big) \tag{3.8}$$

$$= \frac{1}{m_{ij}(\sum_\ell W_\ell)^2}\Big(W_k^{ij} \sum_{\ell\neq k}(W_\ell^{ij} + W_\ell^{\sim ij}) - (W_k^{ij} + W_k^{\sim ij}) \sum_{\ell\neq k} W_\ell^{ij}\Big) \tag{3.9}$$

$$= \frac{1}{m_{ij}(\sum_\ell W_\ell)^2}\Big(W_k^{ij} \sum_{\ell\neq k} W_\ell^{\sim ij} - W_k^{\sim ij} \sum_{\ell\neq k} W_\ell^{ij}\Big), \tag{3.10}$$

resulting in (3.6). ∎

The sign identities (3.5) and (3.6) characterize how the network risk at patch k changes as a function of the movement from patch j to patch i. If more information on the movement network is provided, the exact sign of $\frac{du_k}{dm_{ij}}$ may be able to be determined. If patch k is the head of the altered arc $j \to i$ (i.e., $j = k$), then the sign of the change in the network risk $\frac{du_k}{dm_{ij}}$ is determined in the following result, regardless of the network structure.

THEOREM 3.4. *For any given k, i, $i \neq k$, $\frac{du_k}{dm_{ik}} < 0$.*

Proof. Since there is no spanning in-tree rooted at k that contains the arc $k \to i$ (i.e., leaving the root vertex k), $W_k^{ij} = 0$. It follows from the irreducibility of M that there exists at least one spanning in-tree rooted at k, which certainly does not contain the arc $k \to i$; thus $W_k^{\sim ik} > 0$. If $m_{ik} > 0$, then there exists at least one vertex $\ell \neq k$ at which a spanning in-tree containing $k \to i$ is rooted, and hence $W_\ell^{ik} > 0$. It follows from (3.6) that $\frac{du_k}{dm_{ik}} < 0$.

If $m_{ik} = 0$, then (3.5) can be utilized to establish the result. Specifically, there is no spanning forest of two components where both are rooted at k, which is reflected in our convention that $\det(L_{(ij,kk)}) = 0$. Similarly, the irreducibility of M implies that $W_k > 0$ and $|\det(L_{(ij,\ell k)})| > 0$ for some $\ell \neq k$. ∎

Notice that none of the in-trees rooted at k include the arc $k \to i$, so any increase of m_{ik} does not alter W_k but increases all other $W_\ell, \ell \neq k$. Consequently, all terms in the first sum of (3.5) and (3.6) vanish, as shown in the proof of Theorem 3.4. In contrast, perturbations of m_{kj} change W_k and other $W_\ell, \ell \neq k$, which requires more discussion.

If patch k is the tail of the altered arc $j \to i$ (i.e., $k = i$), and the restriction is added that the only path from j to k is the arc $j \to k$, then the proof of the following result proceeds by an analysis similar to that used to prove Theorem 3.4.

THEOREM 3.5. *For any given k, j, $j \neq k$, if the arc $j \to k$ is the only path from j to k, then $W_k^{\sim kj} = 0$, and $\frac{du_k}{dm_{kj}} > 0$.*

In section 4, we generalize Theorem 3.5 by using the group inverse to remove the restriction on the number of paths from j to k.

4. Algebraic method: Computing the group inverse. Suppose that L is an irreducible Laplacian matrix with zero column sums as in (2.1). Recall from section 2 that there is a unique group inverse $L^\#$ such that $LL^\# = L^\#L$, $LL^\#L = L$, and $L^\#LL^\# = L^\#$. The left and right null spaces of L are necessarily one-dimensional and are spanned by $\mathbb{1}^\top$ and u, respectively, where $u = (u_1, \ldots, u_n)^T$ is the right null vector of L, normalized so that $\mathbb{1}^\top u = \sum_{i=1}^n u_i = 1$. From Corollary 7.2.1 of [7], it now follows that $L^\#L = I - u\mathbb{1}^\top$.

Consider a perturbation $\tilde{L} = L + E$ of L such that $\tilde{L}$ is also a singular and irreducible M-matrix with $\mathbb{1}^\top\tilde{L} = 0$. We seek the normalized right null vector of $\tilde{L}$, i.e., the vector $\tilde{u}$ such that $\tilde{L}\tilde{u} = 0$ and $\mathbb{1}^\top\tilde{u} = 1$. Since $(L + E)\tilde{u} = 0$, we have $L^\#(L + E)\tilde{u} = 0$, and hence $(I - u\mathbb{1}^\top)\tilde{u} + L^\#E\tilde{u} = 0$. Thus $(I + L^\#E)\tilde{u} = u$. Since $I + L^\#E$ is invertible (see [34] or Lemma 5.3.1 in [28]), this gives

$$\tilde{u} = \left(I + L^\#E\right)^{-1}u. \tag{4.1}$$

At the end of this section, we provide an explicit expression for $L^\#$.

The following technical results (see, e.g., [24, p. 19] and [35, p. 475]) are useful in proving Theorem 4.2 below.

LEMMA 4.1. *Let x and y be column vectors of dimension n; then we have $\det(I+xy^\top) = 1+y^\top x$. If, in addition, $y^\top x \neq -1$, then $(I+xy^\top)^{-1} = I-\frac{1}{1+y^\top x}xy^\top$.*

Here is one of the main results of this section.

THEOREM 4.2. *Let L be an irreducible M-matrix as defined in* (2.1).

(a) *Suppose that $L + \epsilon F$ is an irreducible M-matrix with $\mathbb{1}^\top F = 0$ for all ϵ in a neighborhood of 0. Then the directional derivative of u with respect to F is $-L^\#Fu$.*

(b) *Perturb $m_{ij} \to m_{ij} + \epsilon$ (where $\epsilon \geq 0$ when $m_{ij} = 0$) with $1 \leq i \neq j \leq n$, and denote the corresponding right null vector for the Laplacian (normalized to have sum 1) by $\tilde{u}$. Then for $k = 1, \ldots, n$,*

$$\tilde{u}_k - u_k = -\frac{\epsilon\, u_j e_k^\top L^\#(e_j - e_i)}{1 + \epsilon\, e_j^\top L^\#(e_j - e_i)} = -\frac{\epsilon u_j(L^\#_{kj} - L^\#_{ki})}{1 + \epsilon(L^\#_{jj} - L^\#_{ji})}. \tag{4.2}$$

Moreover,

$$\frac{du_k}{dm_{ij}} = -u_j e_k^\top L^\#(e_j - e_i) = -u_j(L^\#_{kj} - L^\#_{ki}), \quad k = 1, \ldots, n, \tag{4.3}$$

and

$$\frac{1}{u_j}\frac{du_k}{dm_{ij}} = -\frac{1}{u_i}\frac{du_k}{dm_{ji}}, \quad k = 1, \ldots, n.$$

Proof. (a) For ϵ sufficiently small,

$$\left(I+\epsilon L^{\#}F\right)^{-1} = I - \epsilon L^{\#}F + O(\epsilon^2). \tag{4.4}$$

Taking $E=\epsilon F$ in (4.1) and using (4.4) yields

$$\tilde{u} = (I+L^{\#}E)^{-1}u = \left(I-\epsilon L^{\#}F\right)u + O(\epsilon^2) = u - \epsilon L^{\#}Fu + O(\epsilon^2). \tag{4.5}$$

Hence $\lim_{\epsilon\to 0}\frac{\tilde{u}-u}{\epsilon} = -L^{\#}Fu$, as desired.

(b) Set $E=\epsilon(-e_i+e_j)e_j^{\top}$. From (4.1), it follows that $\tilde{u}=\left(I+L^{\#}E\right)^{-1}u$, and Lemma 4.1 gives $\left(I+L^{\#}E\right)^{-1} = I - \frac{\epsilon}{1+\epsilon e_j^{\top}L^{\#}(-e_i+e_j)}L^{\#}(-e_i+e_j)e_j^{\top}$. Observe that since $I+\epsilon L^{\#}(-e_i+e_j)e_j^{\top}$ is invertible, $1+\epsilon e_j^{\top}L^{\#}(-e_i+e_j) = \det(I+\epsilon L^{\#}(-e_i+e_j)e_j^{\top}) \neq 0$, following Lemma 4.1. The conclusions now readily follow. ∎

Next we discuss how to find $L^{\#}$. From the hypotheses on L, it is easy to see that L may be partitioned as

$$L = \left(\begin{array}{c|c} \bar{\mathbb{1}}^{\top}z & -\bar{\mathbb{1}}^{\top}B \\ \hline -z & B \end{array}\right),$$

where the submatrix B of L is an $(n-1)\times(n-1)$ invertible matrix, u_1 is the first entry of u, $\bar{u}=(u_2,\ldots,u_n)^{\top}$, $z=\frac{1}{u_1}B\bar{u}$, and $\bar{\mathbb{1}}$ is the all ones column vector of dimension $n-1$.

It follows from Observation 2.3.4 of [28] that

$$L^{\#} = (\bar{\mathbb{1}}^{\top}B^{-1}\bar{u})\,u\mathbb{1}^{\top} + \left(\begin{array}{c|c} 0 & -u_1\bar{\mathbb{1}}^{\top}B^{-1} \\ \hline -B^{-1}\bar{u} & B^{-1}-B^{-1}\bar{u}\bar{\mathbb{1}}^{\top}-\bar{u}\bar{\mathbb{1}}^{\top}B^{-1} \end{array}\right). \tag{4.6}$$

Let $\bar{e}_j$ denote the unit column vector in $\mathbb{R}^{n-1}$ with all zero entries except the jth entry, which is one. Suppose that $1\le i<j\le n$; partitioning out the first entry as above gives

$$L^{\#}(e_j-e_i) = \begin{cases} \left(\begin{array}{c} -u_1\bar{\mathbb{1}}^{\top}B^{-1}\bar{e}_{j-1} \\ \hline B^{-1}\bar{e}_{j-1}-\bar{u}\bar{\mathbb{1}}^{\top}B^{-1}\bar{e}_{j-1} \end{array}\right) & \text{if} \quad i=1, \\ \left(\begin{array}{c} -u_1\bar{\mathbb{1}}^{\top}B^{-1}(\bar{e}_{j-1}-\bar{e}_{i-1}) \\ \hline B^{-1}(\bar{e}_{j-1}-\bar{e}_{i-1})-\bar{u}\bar{\mathbb{1}}^{\top}B^{-1}(\bar{e}_{j-1}-\bar{e}_{i-1}) \end{array}\right) & \text{if} \quad 2\le i\le n. \end{cases} \tag{4.7}$$

From (4.7), we find that $e_1^{\top}L^{\#}(e_1-e_j)>0, j=2,\ldots,n$. The rows and columns of L can be simultaneously permuted to place any index in the first position, and hence

$$L^{\#}_{jj} - L^{\#}_{ji} > 0,\ i,j=1,\ldots,n,\ i\neq j. \tag{4.8}$$

Suppose that $1\le i<j\le n$. If we perturb $m_{ij}\to m_{ij}+\epsilon$ (where $\epsilon\ge 0$ when $m_{ij}=0$), it follows from (4.2) and (4.7) that

$$\tilde{u}_1 - u_1 = \begin{cases} \dfrac{\epsilon u_1 u_j \bar{\mathbb{1}}^{\top}B^{-1}\bar{e}_{j-1}}{1+\epsilon\bar{e}_{j-1}^{\top}\left(B^{-1}\bar{e}_{j-1}-\bar{u}\bar{\mathbb{1}}^{\top}B^{-1}\bar{e}_{j-1}\right)}, & i=1, \\ \dfrac{\epsilon u_1 u_j \bar{\mathbb{1}}^{\top}B^{-1}(\bar{e}_{j-1}-\bar{e}_{i-1})}{1+\epsilon\bar{e}_{j-1}^{\top}\left[B^{-1}(\bar{e}_{j-1}-\bar{e}_{i-1})-\bar{u}\bar{\mathbb{1}}^{\top}B^{-1}(\bar{e}_{j-1}-\bar{e}_{i-1})\right]}, & 2\le i\le n. \end{cases}$$

For $2 \le \ell \le n$, we have

$$\tilde{u}_\ell - u_\ell = \begin{cases} -\dfrac{\epsilon u_j \bar{e}_{\ell-1}^\top \left(B^{-1}\bar{e}_{j-1} - \bar{u}\bar{\mathbb{1}}^\top B^{-1}\bar{e}_{j-1}\right)}{1+\epsilon\bar{e}_{j-1}^\top \left(B^{-1}\bar{e}_{j-1} - \bar{u}\bar{\mathbb{1}}^\top B^{-1}\bar{e}_{j-1}\right)}, & i = 1, \\ -\dfrac{\epsilon u_j \bar{e}_{\ell-1}^\top \left[B^{-1}(\bar{e}_{j-1} - \bar{e}_{i-1}) - \bar{u}\bar{\mathbb{1}}^\top B^{-1}(\bar{e}_{j-1} - \bar{e}_{i-1})\right]}{1+\epsilon\bar{e}_{j-1}^\top \left[B^{-1}(\bar{e}_{j-1} - \bar{e}_{i-1}) - \bar{u}\bar{\mathbb{1}}^\top B^{-1}(\bar{e}_{j-1} - \bar{e}_{i-1})\right]}, & 2 \le i \le n. \end{cases}$$

Remark 4.1. By considering (4.3) and (4.8) for the cases $j = k$ and $i = k$, we find an alternate proof for Theorem 3.4 and an extension of Theorem 3.5 that goes through without the path restriction.

5. Applications to specific networks. In this section, we apply our general results to two different networks: a star network for human transport between one hub and several leaves, and a path network for communities along a river.

5.1. Star network. First, we consider a star network with vertex 1 as the hub and $2, 3, \ldots, n$ as leaf vertices, with corresponding weights $m_{1j}, m_{j1} > 0, j = 2, \ldots, n$. Assuming that a new arc from leaf $j > 1$ to leaf $i > 1$ is added, the following result shows that the direction of change of the network risk u_k at any other vertex (i.e., $k \ne i$, $k \ne j$) depends only on m_{1i} and m_{1j}.

THEOREM 5.1. *For a star network, let i, j be any two distinct leaf vertices, and let k be another vertex. Then* $\operatorname{sgn}(\frac{du_k}{dm_{ij}}) = \operatorname{sgn}(m_{1i} - m_{1j})$.

To illustrate both combinatorial and algebraic methods from sections 3 and 4, we prove the above result using two different approaches.

Combinatorial proof of Theorem 5.1. By Theorem 3.3, it suffices to determine the sign of

$$W_k^{ij} \sum_{\ell \ne k} W_\ell^{\sim ij} - W_k^{\sim ij} \sum_{\ell \ne k} W_\ell^{ij}, \tag{5.1}$$

which involves the weights of certain specific spanning rooted trees. As depicted in Figure 2, $W_k^{ij} = m_{k1}m_{1i}m_{ij}\prod_s m_{1s}$ and $W_k^{\sim ij} = m_{k1}m_{1i}m_{1j}\prod_s m_{1s}$, where s takes all values except $1, k, i, j$, corresponding to the unique spanning in-tree rooted at k that contains the arc $j \to i$ and does not contain the arc $j \to i$, respectively. Now we consider spanning in-trees rooted at $\ell \ne k$, containing $j \to i$ or not, which contributes terms appearing in the sums of (5.1). Specifically, we consider three cases: $\ell = i$, $\ell = j$, and all other possible values (i.e., $\ell = r$, where $r \ne k, i, j$). As depicted in Figure 2, $W_i^{\sim ij} = m_{i1}m_{1j}m_{1k}\prod_s m_{1s}$, $W_j^{\sim ij} = m_{j1}m_{1i}m_{1k}\prod_s m_{1s}$, $W_r^{\sim ij} = m_{r1}m_{1i}m_{1j}m_{1k}\prod_s m_{1s}/m_{1r}$; $W_i^{ij} = m_{i1}m_{ij}m_{1k}\prod_s m_{1s} + m_{ij}m_{j1}m_{1k}\prod_s m_{1s}$, $W_j^{ij} = 0$, $W_r^{ij} = m_{r1}m_{1i}m_{ij}m_{1k}\prod_s m_{1s}/m_{1r}$. Here s takes all values except $1, k, i, j$, and notice that there are two spanning in-trees rooted at i containing $j \to i$, while no spanning in-tree rooted at j contains $j \to i$. There is immediate cancellation in (5.1)

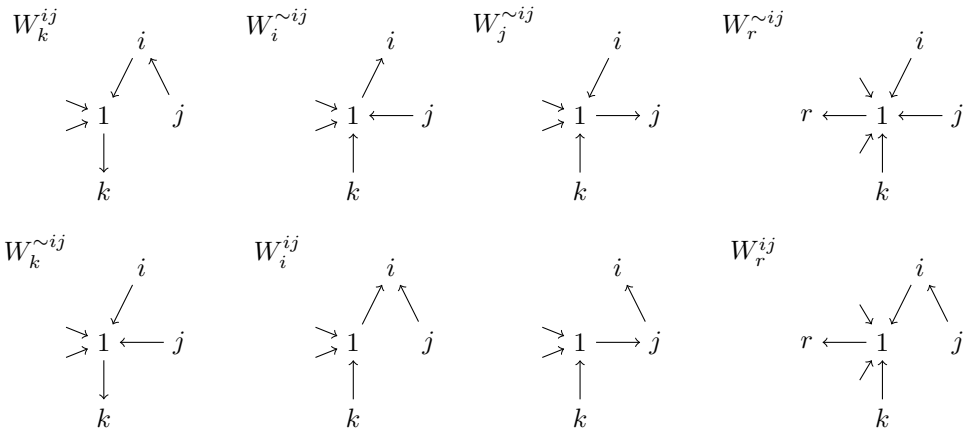

FIG. 2. *Spanning rooted trees with certain specific restrictions in a star network (1 is the hub). Notice that there is no spanning in-tree rooted at j that contains the arc $j \to i$, so $W_j^{ij} = 0$.*

since $W_k^{ij} W_r^{\sim ij} = W_k^{\sim ij} W_r^{ij}$ for all r. After simplification, (5.1) becomes

$$\begin{aligned}
&W_k^{ij} \sum_{\ell \neq k} W_\ell^{\sim ij} - W_k^{\sim ij} \sum_{\ell \neq k} W_\ell^{ij} = W_k^{ij}[W_i^{\sim ij} + W_j^{\sim ij}] - W_k^{\sim ij}[W_i^{ij} + W_j^{ij}] \\
&= m_{k1} m_{1i} m_{ij} \prod_s m_{1s} \Big[m_{i1} m_{1j} m_{1k} \prod_s m_{1s} + m_{j1} m_{1i} m_{1k} \prod_s m_{1s} \Big] \\
&\quad - m_{k1} m_{1i} m_{1j} \prod_s m_{1s} \Big[m_{i1} m_{ij} m_{1k} \prod_s m_{1s} + m_{ij} m_{j1} m_{1k} \prod_s m_{1s} \Big] \\
&= m_{k1} m_{1i} m_{j1} m_{1k} m_{ij} \Big(\prod_s m_{1s} \Big)^2 (m_{1i} - m_{1j}),
\end{aligned}$$

completing the proof. ∎

Algebraic proof of Theorem 5.1. Consider a star network with vertex 1 as the hub, and $2, 3, \ldots, n$ as leaf vertices. From the hypothesis,

$$L = \begin{pmatrix} \sum_{i \neq 1} m_{i1} & -m_{12} & -m_{13} & \ldots & -m_{1n} \\ -m_{21} & m_{12} & 0 & \ldots & 0 \\ -m_{31} & 0 & m_{13} & \ldots & 0 \\ \vdots & \vdots & & & \\ -m_{n1} & 0 & 0 & \ldots & m_{1n} \end{pmatrix}. \tag{5.2}$$

For concreteness, consider $i = 2$ and $j = 3$. It follows from (4.3) that

$$\frac{du}{dm_{23}} = -u_3 L^{\#}(-e_2 + e_3). \tag{5.3}$$

To determine the sign of $\frac{du}{dm_{23}}$, we need to compute the right-hand side of (5.3). As $u_3 > 0$, $sgn(\frac{du}{dm_{23}}) = sgn(-L^{\#}(-e_2 + e_3))$. Since $B = \mathrm{diag}(m_{12}, \ldots, m_{1n})$ is diagonal,

$u_1 \bar{\mathbb{1}}^\top B^{-1}(-\bar{e}_1 + \bar{e}_2) = u_1\left(-\frac{1}{m_{12}} + \frac{1}{m_{13}}\right)$, which implies that

$$(B^{-1} - \bar{u}\bar{\mathbb{1}}^\top B^{-1})(-\bar{e}_1 + \bar{e}_2) = \begin{pmatrix} -\frac{1}{m_{12}} \\ \frac{1}{m_{13}} \\ 0 \\ \vdots \\ 0 \end{pmatrix} - \begin{pmatrix} u_2 \\ u_3 \\ u_4 \\ \vdots \\ u_n \end{pmatrix}\left(-\frac{1}{m_{12}} + \frac{1}{m_{13}}\right).$$

So,

$$-L^{\#}(-e_2 + e_3) = -\begin{pmatrix} -u_1\left(-\frac{1}{m_{12}} + \frac{1}{m_{13}}\right) \\ \begin{pmatrix} -\frac{1}{m_{12}} \\ \frac{1}{m_{13}} \\ 0 \\ \vdots \\ 0 \end{pmatrix} - \begin{pmatrix} u_2 \\ u_3 \\ u_4 \\ \vdots \\ u_n \end{pmatrix}\left(-\frac{1}{m_{12}} + \frac{1}{m_{13}}\right) \end{pmatrix}.$$

Thus,

$$\begin{aligned}
&sgn(\tilde{u}_1 - u_1) = sgn(m_{12} - m_{13}),\\
&sgn(\tilde{u}_2 - u_2) = -sgn\Big(\frac{-m_{13} - u_2(m_{12} - m_{13})}{m_{12}m_{13}}\Big) = sgn(m_{13} + u_2(m_{12} - m_{13})),\\
&sgn(\tilde{u}_3 - u_3) = -sgn\Big(\frac{m_{12} - u_3(m_{12} - m_{13})}{m_{12}m_{13}}\Big) = sgn(-m_{12} + u_3(m_{12} - m_{13})),\\
&sgn(\tilde{u}_\ell - u_\ell) = sgn\Big(\frac{u_\ell(m_{12} - m_{13})}{m_{12}m_{13}}\Big) = sgn(m_{12} - m_{13}),\ \ell = 4, \ldots, n. \qquad \square
\end{aligned}$$

COROLLARY 5.2. *For a star network with vertex* 1 *as the hub, the direction of change of the network risk* u_k *is given by the following:*

$$\begin{aligned}
&sgn\left(\frac{du_k}{dm_{ij}}\right) = sgn(m_{1i} - m_{1j}), \quad k \neq i, j, i \neq 1, j \neq 1,\\
&sgn\left(\frac{du_i}{dm_{ij}}\right) > 0, sgn\left(\frac{du_j}{dm_{ij}}\right) < 0.
\end{aligned} \tag{5.4}$$

5.2. River network. Consider a path network with vertices labeled $1, 2, 3, \ldots, n$ consecutively located along a river, where 1 denotes the vertex that is farthest upstream and n is the vertex that is farthest downstream. Suppose further that the associated movement matrix M is constant along its superdiagonal and constant along its subdiagonal. (This corresponds to constant dispersal rates for upstream and downstream movements.) The corresponding Laplacian matrix $\hat{L}$ is given by

$$\hat{L} = \begin{pmatrix} a & -b & 0 & \cdots & 0 & 0 \\ -a & a+b & -b & \cdots & 0 & 0 \\ 0 & -a & a+b & \cdots & 0 & 0 \\ \vdots & \vdots & & & & \\ 0 & 0 & 0 & \cdots & a+b & -b \\ 0 & 0 & 0 & \cdots & -a & b \end{pmatrix} \tag{5.5}$$

for $a > 0$ and $b > 0$. It suffices to consider the case when $a \geq b$; see supplementary material section (B) for a justification. Henceforth we restrict our attention to the case when $a \geq b$.

Setting $\alpha = \frac{a}{b}$ yields

$$\hat{L} = b \begin{pmatrix} \alpha & -1 & 0 & \cdots & 0 & 0 \\ -\alpha & \alpha+1 & -1 & \cdots & 0 & 0 \\ 0 & -\alpha & \alpha+1 & \cdots & 0 & 0 \\ \vdots & \vdots & & & & \\ 0 & 0 & 0 & \cdots & \alpha+1 & -1 \\ 0 & 0 & 0 & \cdots & -\alpha & 1 \end{pmatrix} := bL. \tag{5.6}$$

Our assumption that $a \geq b$ gives $\alpha \geq 1$, and we note that this fits into our interpretation of 1 being an upstream vertex and n being a downstream vertex. It is readily verified that the vector

$$u = (u_1, u_2, \ldots, u_n)^\top = \frac{1}{\sum_{\ell=0}^{n-1} \alpha^\ell}(1, \alpha, \alpha^2, \ldots, \alpha^{n-1})^\top$$

is the right null vector of L normalized so that $\mathbb{1}^\top u = 1$. Let B denote the principal submatrix of L formed by deleting the first row and column. A proof by induction on n shows that the (k, j) entry of B^{-1} is given by

$$\bar{e}_k^\top B^{-1} \bar{e}_j = \begin{cases} 1 + \alpha + \alpha^2 + \cdots + \alpha^{k-1}, & 1 \leq k \leq j \leq n-1, \\ \alpha^{k-j}(1 + \alpha + \alpha^2 + \cdots + \alpha^{j-1}), & 1 \leq j < k \leq n-1. \end{cases}$$

It can be shown by induction on n that the sum of the entries in column j of B^{-1} is

$$\bar{\mathbb{1}}^\top B^{-1} \bar{e}_j = j \sum_{\ell=0}^{n-j-1} \alpha^\ell + \sum_{\ell=n-j}^{n-2} (n-1-\ell)\alpha^\ell, \quad j = 1, 2, \ldots, n-1,$$

where the empty sum is interpreted as zero.

The following is straightforward.

LEMMA 5.3. *Suppose that $m \geq 0$ and $n \in \mathbb{N}$. Then*

$$\left(\sum_{\ell=0}^{m} \alpha^\ell\right)\left(\sum_{\ell=0}^{n-1} \alpha^\ell\right) = \sum_{\ell=0}^{m} (\ell+1)\alpha^\ell + (m+1) \sum_{\ell=m+1}^{n-1} \alpha^\ell + \sum_{\ell=n}^{n+m-1} (n+m-\ell)\alpha^\ell.$$

The following can be deduced from (4.7) and our expression for B^{-1}.

LEMMA 5.4. *For a path network, if $1 \leq i < j \leq n$, then*

$$L^{\#}_{jj} - L^{\#}_{ji} = \frac{\sum_{\ell=0}^{j-i-1}(\ell+1)\alpha^\ell + (j-i)\sum_{\ell=j-i}^{j-2} \alpha^\ell}{\sum_{\ell=0}^{n-1} \alpha^\ell}.$$

Lemmas 5.3 and 5.4, along with (4.7), establish the following result.

THEOREM 5.5. *On a path network, if $1 \leq k \leq j \leq n$, then*

$$\begin{aligned} &e_k^\top L^{\#}(e_j - e_1) \\ &= \frac{1}{\sum_{\ell=0}^{n-1} \alpha^\ell}\left(\sum_{\ell=0}^{k-2}(\ell+1)\alpha^\ell - (j-k)\sum_{\ell=k-1}^{n+k-j-1} \alpha^\ell - \sum_{\ell=n-j+k}^{n-2} (n-\ell-1)\alpha^\ell\right). \end{aligned}$$

For $j < k \le n$,

$$e_k^\top L^\# (e_j - e_1) = \alpha^{k-j} e_j^\top L^\# (e_j - e_1) = \frac{\alpha^{k-j}}{\sum_{\ell=0}^{n-1} \alpha^\ell} \left(\sum_{\ell=0}^{j-2} (\ell+1)\alpha^\ell \right).$$

Theorem 5.5 yields the following result.

COROLLARY 5.6. *For* $1 \le k \le j-1$,

$$(e_{k+1}^\top - e_k^\top) L^\# (e_j - e_1) = \frac{\alpha^{k-1}}{\sum_{\ell=0}^{n-1} \alpha^\ell} \left(j + \sum_{\ell=1}^{n-j} \alpha^\ell \right) > 0.$$

For $j \le k \le n-1$,

$$(e_{k+1}^\top - e_k^\top) L^\# (e_j - e_1) = \frac{\alpha^{k-j}}{\sum_{\ell=0}^{n-1} \alpha^\ell} \left(\sum_{\ell=0}^{j-2} (\ell+1)\alpha^\ell \right) (\alpha - 1) > 0.$$

Remark 5.1. Set $\tilde{L} = L + \epsilon(e_j - e_1)e_j^\top$ with $1 < j \le n$ and $\epsilon > 0$ so that $\tilde{u} - u = -cL^\#(e_j - e_1)$, where $c = \frac{\epsilon u_j}{1+\epsilon(L^\#_{jj} - L^\#_{j1})} > 0$ by Theorem 4.2(b). By Theorem 5.5, $\tilde{u}_1 - u_1 > 0$ and $\tilde{u}_k - u_k < 0, j \le k \le n$. It follows from Corollary 5.6 that $\tilde{u}_k - u_k$ is decreasing in k if $\alpha > 1$. If $\alpha = 1$, $\tilde{u}_k - u_k$ is decreasing in k for $1 \le k \le j$ and constant for $j \le k \le n$.

Next we consider $L^\#(e_j - e_i)$ for $j, i > 1$. The proofs again rely on (4.7) and our expression for B^{-1}.

LEMMA 5.7. *For a path network with* $2 \le i < j \le n$,

$$\bar{e}_k^\top B^{-1} (\bar{e}_{j-1} - \bar{e}_{i-1}) = \begin{cases} 0 & \text{if } 1 \le k \le i-1, \\ \sum_{\ell=0}^{k-i} \alpha^\ell & \text{if } i-1 < k \le j-1, \\ \alpha^{k-j+1} \sum_{\ell=0}^{j-i} \alpha^\ell & \text{if } j-1 < k \le n. \end{cases}$$

THEOREM 5.8. *On a path network, if* $2 \le i < j \le n$, *then*

$$e_k^\top L^\# (e_j - e_i) = -\frac{\alpha^{k-1}}{\sum_{\ell=0}^{n-1} \alpha^\ell} \left((j-i) \sum_{\ell=0}^{n-j} \alpha^\ell + \sum_{\ell=n-j+1}^{n-i-1} (n-i-\ell)\alpha^\ell \right)$$

for $1 \le k \le i$. *For* $i < k \le j$,

$$e_k^\top L^\# (e_j - e_i) = \frac{1}{\sum_{\ell=0}^{n-1} \alpha^\ell} \left(\sum_{\ell=0}^{k-i-1} (\ell+1)\alpha^\ell + (k-i) \sum_{\ell=k-i}^{k-2} \alpha^\ell \right.$$
$$\left. - (j-k) \sum_{\ell=k-1}^{n+k-j-1} \alpha^\ell - \sum_{\ell=n-j+k}^{n-2} (n-1-\ell)\alpha^\ell \right).$$

For $j < k \le n$, $e_k^\top L^\# (e_j - e_i) = \alpha^{k-j} e_j^\top L^\# (e_j - e_i) = \frac{\alpha^{k-j}}{\sum_{\ell=0}^{n-1} \alpha^\ell} \left(\sum_{\ell=0}^{j-i-1} (\ell+1)\alpha^\ell + (j-i) \sum_{\ell=j-i}^{j-2} \alpha^\ell \right)$.

COROLLARY 5.9. *If* $2 \le i < j \le n$, *then*

$$(e_{k+1} - e_k^\top)L^\#(e_j - e_i) = \begin{cases} -\dfrac{\alpha^{k-1}}{\sum_{\ell=0}^{n-1}\alpha^\ell}\left((j-i)\sum_{\ell=0}^{n-j}\alpha^\ell + \sum_{\ell=n-j+1}^{n-i-1}(n-i-\ell)\alpha^\ell\right)(\alpha-1) \ge 0, & 1 \le k \le i-1, \\ \dfrac{1}{\sum_{\ell=0}^{n-1}\alpha^\ell}\left(\sum_{\ell=0}^{i-2}\alpha^\ell + (j-i+1)\alpha^{i-1} + \sum_{\ell=i}^{n+i-j-1}\alpha^\ell\right) > 0, & k = i, \\ \dfrac{1}{\sum_{\ell=0}^{n-1}\alpha^\ell}\left(\sum_{\ell=k-i}^{k-2}\alpha^\ell + (j-i+1)\alpha^{k-1} + \sum_{\ell=k}^{n+k-j-1}\alpha^\ell\right) > 0, & i < k \le k+1 \le j, \\ \dfrac{\alpha^{k-j}}{\sum_{\ell=0}^{n-1}\alpha^\ell}\left(\sum_{\ell=0}^{j-2}(l\ell+1)\alpha^\ell\right)(\alpha-1) \ge 0, & j \le k \le n-1. \end{cases}$$

Remark 5.2. Let $2 \le i < j \le n$ and $\epsilon > 0$. Set $\tilde{L} = L + \epsilon(e_j - e_i)e_j^\top$. It follows from Theorem 4.2(b) that

$$\tilde{u} - u = -cL^\#(e_j - e_i), \tag{5.7}$$

where $c = \frac{\epsilon u_j}{1+\epsilon(L^\#_{jj} - L^\#_{ji})} > 0$ (observe that $L^\#_{jj} - L^\#_{ji} > 0$ by (4.8)). In view of Theorem 5.8, we see that

$$\tilde{u}_k - u_k = \begin{cases} \dfrac{c\alpha^{k-1}}{\sum_{\ell=0}^{n-1}\alpha^\ell}\left((j-i)\sum_{\ell=0}^{n-j}\alpha^\ell + \sum_{\ell=0}^{n-i-1}(n-i-\ell)\alpha^\ell\right) > 0, & 1 \le k \le i, \\ \dfrac{-c\alpha^{k-j}}{\sum_{\ell=0}^{n-1}\alpha^\ell}\left(\sum_{\ell=0}^{j-i-1}(\ell+1)\alpha^\ell + (j-i)\sum_{\ell=j-i}^{j-2}\alpha^\ell\right) < 0, & j \le k \le n. \end{cases}$$

Observe that if $i \ge 2$ and $1 \le k \le n-1, (\tilde{u}_{k+1} - u_{k+1}) - (\tilde{u}_k - u_k) = -c(e_{k+1} - e_k^\top)L^\#(e_j - e_i)$. It now follows from Corollary 5.9 that if $\alpha > 1$, then $(\tilde{u}_{k+1} - u_{k+1}) - (\tilde{u}_k - u_k) < 0$. Hence, if $\alpha > 1$, then $\tilde{u}_k - u_k$ is decreasing as a function of k for $1 \le k \le n$.

Assume that a new arc from vertex j to vertex i is added, where $i < j$; the following result shows that the network risk u_k decreases at all vertices downstream from j and increases at all vertices upstream from i. The result readily follows from Theorems 4.2 and 5.8.

THEOREM 5.10. *Consider a path network, and suppose that* $1 \le i < j \le n$. *For any* $k \le i$, $\operatorname{sgn}(\frac{du_k}{dm_{ji}}) < 0$, *while for any* $j < k$, $\operatorname{sgn}(\frac{du_k}{dm_{ji}}) > 0$.

For the vertices k between j and i (i.e., $i < k < j$), the change of the network risk u_k depends on the position of the vertices as well as the magnitude of m_{ij}.

We now revisit the toy model of a path graph network described in section 1.

Example 1. In this example we show how the results developed in section 4 yield insight into the toy example presented in Figure 1. We suppose that the time scale of movement greatly exceeds that of the disease dynamics, so that the asymptotic approximation $\mathcal{R}_0 = \sum_{k=1}^4 u_k q_k$ applies, where u denotes the null vector of the Laplacian

matrix L, normalized so that $\sum_{k=1}^{4} u_k = 1$. Taking $\alpha = 1$ yields

$$L = \begin{pmatrix} 1 & -1 & 0 & 0 \\ -1 & 2 & -1 & 0 \\ 0 & -1 & 2 & -1 \\ 0 & 0 & -1 & 1 \end{pmatrix},$$

and

$$L^{\#} = \frac{1}{8} \begin{pmatrix} 7 & 1 & -3 & -5 \\ 1 & 3 & -1 & -3 \\ -3 & -1 & 3 & 1 \\ -5 & -3 & 1 & 7 \end{pmatrix}.$$

A bypass from vertex 1 to vertex 3 corresponds to the perturbing matrix $E = m_{31}(e_1 - e_3)e_1^{\top}$, and a computation now reveals that the normalized null vector of the perturbed Laplacian matrix is given by

$$\tilde{u} = \frac{1}{4}\mathbb{1} - \frac{m_{31}}{16 + 20m_{31}} \begin{pmatrix} 5 \\ 1 \\ -3 \\ -3 \end{pmatrix}.$$

If the hot spot is at vertex 2, with $q_i = q, i = 1, 3, 4, q_2 = 10q$, then $\mathcal{R}_0 = \sum_{k=1}^{4} \tilde{u}_k q_k = q(\frac{13}{4} - \frac{9m_{31}}{16+20m_{31}})$; evidently this is decreasing and concave down as a function of m_{31}, as is clearly reflected in Figure 1 (left plot) by computing $\mathcal{R}_0$ numerically.

Next, considering a bypass from vertex 2 to vertex 4 (so that E is given by $m_{42}(e_2 - e_4)e_2^{\top}$), an analogous argument shows that

$$\tilde{u} = \frac{1}{4}\mathbb{1} - \frac{m_{42}}{16 + 12m_{42}} \begin{bmatrix} 3 \\ 3 \\ -1 \\ -5 \end{bmatrix}.$$

With vertex 3 as the hot spot and $q_i = q, i = 1, 2, 4, q_3 = 10q$, it now follows that $\sum_{k=1}^{4} \tilde{u}_k q_k = q(\frac{13}{4} + \frac{9m_{42}}{16+12m_{42}})$. Evidently this last term is increasing and concave down as a function of m_{42}, as depicted in Figure 1 (right plot).

Alternatively, as u_k encodes the weights of spanning in-trees rooted at k, as shown in section 3, both bypasses (from vertex 1 to vertex 3 and from vertex 2 to vertex 4) increase u_1 and u_2 but decrease u_3 and u_4. For example, with the bypass from vertex 1 to vertex 3 of weight m_{31}, we have

$$\begin{aligned} u_1 &= \frac{m_{12}m_{23}m_{34}}{\Delta} = \frac{1}{4 + 5m_{31}} = \frac{1}{4} - \frac{\frac{5}{4}m_{31}}{4 + 5m_{31}}, \\ u_2 &= \frac{m_{21}m_{23}m_{34} + m_{23}m_{31}m_{34}}{\Delta} = \frac{1 + m_{31}}{4 + 5m_{31}} = \frac{1}{4} - \frac{\frac{1}{4}m_{31}}{4 + 5m_{31}}, \\ u_3 &= \frac{m_{34}m_{32}m_{21} + m_{34}m_{31}m_{12} + m_{34}m_{31}m_{32}}{\Delta} = \frac{1 + 2m_{31}}{4 + 5m_{31}} = \frac{1}{4} + \frac{\frac{3}{4}m_{31}}{4 + 5m_{31}}, \\ u_4 &= \frac{m_{43}m_{32}m_{21} + m_{43}m_{32}m_{31} + m_{43}m_{31}m_{12}}{\Delta} = \frac{1 + 2m_{31}}{4 + 5m_{31}} = \frac{1}{4} + \frac{\frac{3}{4}m_{31}}{4 + 5m_{31}}, \end{aligned}$$

where Δ is the sum of weights of spanning in-trees rooted at any vertex, that is, $\Delta = m_{12}m_{23}m_{34} + m_{21}m_{23}m_{34} + m_{23}m_{31}m_{34} + m_{34}m_{32}m_{21} + m_{34}m_{31}m_{12} + m_{34}m_{31}m_{32} +$

$m_{43}m_{32}m_{21} + m_{43}m_{32}m_{31} + m_{43}m_{31}m_{12} = 4 + 5m_{31}$. A hot spot at vertex 1 or 2 leads to the decrease of $\mathcal{R}_0$ due to the bypass, while a hot spot at vertex 3 or 4 leads to the increase of $\mathcal{R}_0$.

Example 2. Consider a path network on five vertices with an additional arc from vertex 2 to vertex 4. All other settings are the same as in Example 1. Figure 3 shows how $\mathcal{R}_0$ responds to this addition in the scenarios where the disease hot spot is located at various vertices. It turns out that when vertex 3 is the hot spot, there is no change in $\mathcal{R}_0$ no matter how large the value of m_{24}. When the time scale of movement greatly exceeds that of the disease dynamics, the results of sections 3 and 4 explain Figure 3. For example, the bypass decreases u_1 and u_2 but increases u_4 and u_5. Therefore, a hot spot at vertex 1 or 2 leads to a decrease of $\mathcal{R}_0$ while a hot spot at vertex 4 or 5 leads to an increase of $\mathcal{R}_0$, due to the bypass.

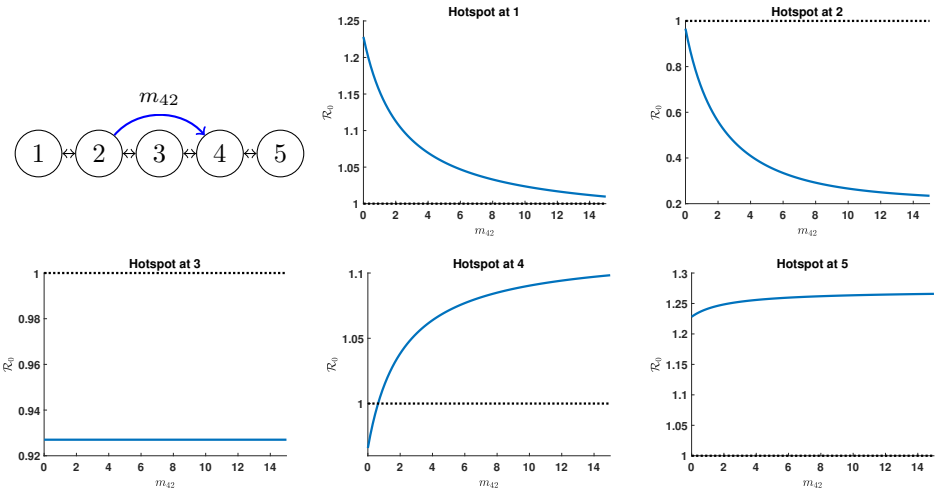

FIG. 3. *The impact of a bypass in a path network of five vertices.*

Motivated by the observation made in Example 2 for the case when vertex 3 is the hot spot, we use the exact network basic reproduction number to prove a general result below, from which the observation is readily recovered.

THEOREM 5.11. *Suppose that M is an irreducible movement matrix and that L is the corresponding Laplacian matrix. Let $c > 0$ and $V = L + cI$. Suppose further that there is a permutation matrix Q and indices i, j such that* (a) *both F and L commute with Q, and* (b) *$Qe_j = e_i$. Then for any $\epsilon > 0$, the basic reproduction numbers corresponding to M and $M + \epsilon(e_j - e_i)e_j^\top$ are equal.*

Proof. Let $E = \epsilon(e_j - e_i)e_j^\top$. The network basic reproduction number corresponding to M is $\rho(FV^{-1})$, while that corresponding to the perturbed network $M + E$ is $\rho(F(V + E)^{-1})$. We have

$$F(V+E)^{-1} = FV^{-1}\Big(I + \epsilon(e_j - e_i)e_j^\top V^{-1}\Big)^{-1}. \tag{5.8}$$

Observe that V is a column diagonally dominant M-matrix. From Lemma 3.14 in Chapter 9 of [5], it follows that the maximum entry in any row of V^{-1} occurs on the

diagonal. In particular, $e_j^\top V^{-1}(e_j - e_i) \geq 0$. It now follows that

$$\left(I + \epsilon(e_j - e_i)e_j^\top V^{-1}\right)^{-1} = I - \frac{\epsilon}{1 + \epsilon e_j^\top V^{-1}(e_j - e_i)}(e_j - e_i)e_j^\top V^{-1}. \tag{5.9}$$

Substituting (5.9) into (5.8) yields

$$\begin{aligned} F(V+E)^{-1} &= FV^{-1}\left[I - \frac{\epsilon}{1 + \epsilon e_j^\top V^{-1}(e_j - e_i)}(e_j - e_i)e_j^\top V^{-1}\right] \\ &= FV^{-1} - \frac{\epsilon FV^{-1}(e_j - e_i)e_j^\top V^{-1}}{1 + \epsilon e_j^\top V^{-1}(e_j - e_i)}. \end{aligned}$$

Next, consider a positive left Perron vector y for FV^{-1}, i.e., $y^\top FV^{-1} = \mathcal{R}_0 y^\top$. Since both F and V commute with Q, so does FV^{-1}. Consequently, $y^\top QFV^{-1}Q^\top = \mathcal{R}_0 y^\top$, implying that $(y^\top Q)FV^{-1} = \mathcal{R}_0(y^\top Q)$. Hence $y^\top Q$ is also a left Perron vector for FV^{-1}. Since that Perron vector is unique up to a scalar multiple, we find that necessarily $y^\top Q = y^\top$. In particular, $y_i = y^\top Qe_j = y^\top e_j = y_j$.

Now consider

$$\begin{aligned} y^\top F(V+E)^{-1} &= y^\top FV^{-1} - \frac{\epsilon y^\top FV^{-1}(e_j - e_i)e_j^\top V^{-1}}{1 + \epsilon e_j^\top V^{-1}(e_j - e_i)} \\ &= \mathcal{R}_0 y^\top - \frac{\epsilon \mathcal{R}_0(y_j - y_i)e_j^\top V^{-1}}{1 + \epsilon e_j^\top V^{-1}(e_j - e_i)} = \mathcal{R}_0 y^\top. \end{aligned}$$

Hence y is a positive left eigenvector of $F(V+E)^{-1}$, (with corresponding eigenvalue $\mathcal{R}_0$), from which it follows that $F(V+E)^{-1}$ has y as a left Perron vector and $\mathcal{R}_0$ as its Perron value. ∎

Remark 5.3. Inspecting the proof of Theorem 5.11, we find that the conclusion holds also for negative values of ϵ, provided that $\epsilon > -m_{ij}$ and $\epsilon > -\frac{1}{e_j^\top V^{-1}(e_j - e_i)}$.

As an application of Theorem 5.11, consider a river network on $2k+1$ vertices with $\alpha = 1$, and suppose that F is the diagonal matrix whose ℓth diagonal entry is 1 for $\ell \neq k+1$ and whose $(k+1)$st diagonal entry is $x > 1$. Setting $V = L + cI$ for some $c > 0$, we see that V and F commute with the "back diagonal" permutation matrix P, where the $(\ell, 2k+2-\ell)$ entry of P is 1 for $\ell = 1, \ldots, 2k+1$. Fix an index $j = 1, \ldots, 2k+1$, and note that $Pe_j = e_{2k+2-j}$. From the above theorem, for any $\epsilon > 0$, the basic reproduction numbers associated with the movement matrices M and $M + \epsilon(e_j - e_{2k+2-j})e_j^\top$ are equal. In particular, for a river network on five vertices with $\alpha = 1$, adding a weighted arc from vertex 4 to vertex 2 does not affect the value of $\mathcal{R}_0$. This justifies the observation made in Example 2 that the hot spot is located at vertex 3.

6. Control strategies. The techniques developed in sections 3 and 4 inform a strategy for controlling invasibility. Given an irreducible movement matrix M, the control strategy corresponds to a perturbation of M, say $M + E$ which is also irreducible and nonnegative. Denoting the corresponding Laplacian matrices and normalized right null vectors by L, u and $\tilde{L}, \tilde{u}$, respectively, we find that the associated network basic reproduction numbers are approximately $\mathcal{R}_0 = \sum_{k=1}^n u_k \mathcal{R}_0^{(k)}$ and $\tilde{\mathcal{R}}_0 = \sum_{k=1}^n \tilde{u}_k \mathcal{R}_0^{(k)}$. Our goal is then to find a suitable perturbing matrix E so as to ensure that $\tilde{\mathcal{R}}_0 - \mathcal{R}_0$ is negative and, ideally, large in absolute value.

From the results in section 4, we find that

$$\tilde{\mathcal{R}}_0 - \mathcal{R}_0 = \sum_{k=1}^{n} (\tilde{u}_k - u_k)\mathcal{R}_0^{(k)} = \sum_{k=1}^{n} e_k^\top ((I + L^\# E)^{-1} - I) u \mathcal{R}_0^{(k)}. \tag{6.1}$$

In particular, for a perturbing matrix E, the effectiveness of the corresponding control strategy in mitigating the invasion can be quantified using (6.1).

In this section, we focus on a restricted set of perturbations: for distinct indices i, j and fixed ϵ, we consider the effect of increasing the movement rate from patch j to patch i from m_{ij} to $m_{ij} + \epsilon$. In this case, (6.1) simplifies considerably: from the results of section 4, it follows that in this restricted setting,

$$\tilde{\mathcal{R}}_0 - \mathcal{R}_0 = -\frac{\epsilon u_j}{1 + \epsilon(L^\#_{jj} - L^\#_{ji})} \sum_{k=1}^{n} (L^\#_{kj} - L^\#_{ki})\mathcal{R}_0^{(k)}. \tag{6.2}$$

Our challenge is then to select the indices i, j so as to minimize the expression

$$-\frac{\epsilon u_j}{1 + \epsilon(L^\#_{jj} - L^\#_{ji})} \sum_{k=1}^{n} (L^\#_{kj} - L^\#_{ki})\mathcal{R}_0^{(k)}. \tag{6.3}$$

We remark here that for $\epsilon > 0$, the expression (6.2) is always valid. However, for negative values of ϵ, another hypothesis is required in order for the derivation of (6.2) to hold. In that case, we need to assume that $-m_{ij} < \epsilon$ (otherwise, there is a danger that the network is no longer strongly connected). Evidently that additional hypothesis is satisfied if, for example, we assume that when ϵ is negative, its absolute value is sufficiently small. For ease of exposition in what follows, we only deal with the case $\epsilon > 0$ in the remainder of this section.

While we focus only on perturbing a single entry in the movement matrix M, note that these special perturbations are building blocks: any admissible perturbation can be written as a linear combination of these restricted perturbations.

From (6.3) it is clear that the specific values of $\mathcal{R}_0^{(k)}, k = 1, \ldots, n$, are needed in order for us to assess the effect on the basic reproduction number of changing m_{ij} to $m_{ij} + \epsilon$. However, we restrict ourselves to the following situation, in which the analysis simplifies even further. Imagine that one patch, say ℓ, is a "hot spot" for the disease, and that the patch reproduction numbers $\mathcal{R}_0^{(k)}, k \neq \ell$, take on a common value. Formally we assume that for some index ℓ, we have $\mathcal{R}_0^{(k)} = r_0$ whenever $k \neq \ell$, with $\mathcal{R}_0^{(\ell)} > r_0$. Then $\tilde{\mathcal{R}}_0 - \mathcal{R}_0 = \sum_{k=1,\ldots,n,k\neq\ell} (\tilde{u}_k - u_k)\mathcal{R}_0^{(k)} + (\tilde{u}_\ell - u_\ell)\mathcal{R}_0^{(\ell)} = r_0 \sum_{k=1,\ldots,n,k\neq\ell} (\tilde{u}_k - u_k) + (\tilde{u}_\ell - u_\ell)\mathcal{R}_0^{(\ell)}$. The fact that $\sum_{k=1}^{n} (\tilde{u}_k - u_k) = 0$ gives

$$\tilde{\mathcal{R}}_0 - \mathcal{R}_0 = (\tilde{u}_\ell - u_\ell)(\mathcal{R}_0^{(\ell)} - r_0). \tag{6.4}$$

For our restricted family of perturbations, we have $\tilde{\mathcal{R}}_0 - \mathcal{R}_0 = -\frac{\epsilon u_j}{1+\epsilon(L^\#_{jj} - L^\#_{ji})}(L^\#_{\ell j} - L^\#_{\ell i})(\mathcal{R}_0^{(\ell)} - r_0)$. Hence it suffices to select the indices i, j that maximize the expression $\frac{u_j}{1+\epsilon(L^\#_{jj} - L^\#_{ji})}(L^\#_{\ell j} - L^\#_{\ell i})$. In subsections 6.1 and 6.2, we revisit the star and river networks and discuss how these perturbations affect the basic reproduction number.

6.1. Star with a hot spot. In what follows, we assume that $\epsilon > 0$, and we consider a special case. We assume that $m_{12} \geq m_{13} \geq \cdots \geq m_{1n}$ and impose the further

assumption that $m_{1k} = m_{k1}, k = 2, \ldots, n$. We note that when this is the case, $u = \frac{1}{n}\mathbb{1}$.

Case 1. *The hot spot is located at the hub (vertex* 1*).* We claim that the best strategy for reducing the infection risk is to increase m_{n1} when $m_{1k} = m_{k1}$ for $2 \le k \le n$. Perturb $m_{1j} \to m_{1j} + \epsilon$ for $\epsilon > 0$ and $1 < j \le n$. Then

$$\begin{aligned}\tilde{u}_1 - u_1 &= -\frac{\epsilon\, u_j e_1^\top L^{\#}(e_j - e_1)}{1 + \epsilon\, e_j^\top L^{\#}(e_j - e_1)} = \frac{\epsilon u_1 u_j \bar{\mathbb{1}}^\top B^{-1}\bar{e}_{j-1}}{1 + \epsilon\bar{e}_{j-1}^\top\big(B^{-1}\bar{e}_{j-1} - \bar{u}\bar{\mathbb{1}}^\top B^{-1}\bar{e}_{j-1}\big)} \\ &= \frac{\epsilon u_1 u_j/m_{1j}}{1 + \epsilon(1-u_j)/m_{1j}} > 0.\end{aligned}$$

Perturb $m_{i1} \to m_{i1} + \epsilon$ for $1 < i \le n$. Since $B^{-1} = \operatorname{diag}(m_{12}, \ldots, m_{1n})$,

$$\begin{aligned}\tilde{u}_1 - u_1 &= -\frac{\epsilon\, u_1 e_1^\top L^{\#}(e_1 - e_i)}{1 + \epsilon\, e_1^\top L^{\#}(e_1 - e_i)} = \frac{\epsilon\, u_1 e_1^\top L^{\#}(e_i - e_1)}{1 - \epsilon\, e_1^\top L^{\#}(e_i - e_1)} = \frac{-\epsilon u_1^2 \bar{\mathbb{1}}^\top B^{-1}\bar{e}_{i-1}}{1 + \epsilon u_1 \bar{\mathbb{1}}^\top B^{-1}\bar{e}_{i-1}} \\ &= -\frac{\epsilon u_1^2/m_{1i}}{1 + \epsilon u_1/m_{1i}} < 0.\end{aligned}$$

Since $u = \frac{1}{n}\mathbb{1}$, this gives

$$\tilde{u}_1 - u_1 = -\frac{1}{n}\frac{\epsilon/(nm_{1i})}{1 + \epsilon/(nm_{1i})}.$$

Since m_{1n} is the smallest among $\{m_{1k} : 2 \le k \le n\}$, the minimum of $\tilde{u}_1 - u_1$ is achieved at $k = n$, i.e.,

$$\min_{2 \le k \le n}(\tilde{u}_1 - u_1) = -\frac{1}{n}\frac{\epsilon/(nm_{1n})}{1 + \epsilon/(nm_{1n})}.$$

This result indicates that the optimal strategy for reducing the infection risk is to increase m_{n1} when $m_{1k} = m_{k1}$ for all k.

Additionally, we claim that in this special case, where only changing weights between leaves is permitted, the best strategy is to increase m_{n2}, as we now show. Perturbing $m_{ij} \to m_{ij} + \epsilon$ for $2 \le i \ne j \le n$, we find that

$$\begin{aligned}\tilde{u}_1 - u_1 &= -\frac{\epsilon\, u_j e_1^\top L^{\#}(e_j - e_i)}{1 + \epsilon\, e_j^\top L^{\#}(e_j - e_i)} \\ &= \frac{\epsilon u_1 u_j \bar{\mathbb{1}}^\top B^{-1}(\bar{e}_{j-1} - \bar{e}_{i-1})}{1 + \epsilon\bar{e}_{j-1}^\top\big[B^{-1}(\bar{e}_{j-1} - \bar{e}_{i-1}) - \bar{u}\bar{\mathbb{1}}^\top B^{-1}(\bar{e}_{j-1} - \bar{e}_{i-1})\big]} \\ &= \frac{\epsilon\frac{1}{n^2}\left(\frac{1}{m_{1j}} - \frac{1}{m_{1i}}\right)}{1 + \epsilon\left(\frac{1}{m_{1j}} - \frac{1}{n}\left(\frac{1}{m_{1j}} - \frac{1}{m_{1i}}\right)\right)} = \frac{\epsilon\frac{1}{n^2}(m_{1i} - m_{1j})}{m_{1i}m_{1j} + \epsilon\frac{1}{n}((n-1)m_{1i} + m_{1j})}.\end{aligned} \tag{6.5}$$

Note that $\tilde{u}_1 - u_1 < 0$ only if $i > j$, and hence this is the only interesting case.

It is straightforward to show that

$$\frac{\epsilon\frac{1}{n^2}(m_{1i} - m_{1j})}{m_{1i}m_{1j} + \epsilon\frac{1}{n}((n-1)m_{1i} + m_{1j})}$$

is increasing in m_{1i} and decreasing in m_{1j}. Thus the minimum is obtained at $i = n$ and $j = 2$. Hence,

$$\min_{1\le j<i\le n}(\tilde{u}_1 - u_1) = \frac{\epsilon\frac{1}{n^2}(m_{1n} - m_{12})}{m_{1n}m_{12} + \epsilon\frac{1}{n}((n-1)m_{1n} + m_{12})},$$

which implies that the most effective strategy for reducing the risk of infection is to increase m_{n2}.

Case 2. *The hot spot is located on a leaf (vertex $\ell \neq 1$).* We claim that the best strategy is to increase m_{n1} when $\frac{m_{1\ell}}{m_{1n}} > n-1$ and $n \neq \ell$, and to increase $m_{1\ell}$ when $\frac{m_{1\ell}}{m_{1n}} < n-1$, as we now show. Perturbing $m_{1\ell} \to m_{1\ell} + \epsilon$ yields

$$\begin{aligned}\tilde{u}_\ell - u_\ell &= -\frac{\epsilon\, u_\ell e_\ell^\top L^\#(e_\ell - e_1)}{1 + \epsilon\, e_\ell^\top L^\#(e_\ell - e_1)} = -\frac{\epsilon u_\ell e_{\ell-1}^\top\big(B^{-1}\bar{e}_{\ell-1} - \bar{u}\bar{\mathbb{1}}^\top B^{-1}\bar{e}_{\ell-1}\big)}{1 + \epsilon\bar{e}_{\ell-1}^\top\big(B^{-1}\bar{e}_{\ell-1} - \bar{u}\bar{\mathbb{1}}^\top B^{-1}\bar{e}_{\ell-1}\big)} \\ &= -\frac{\epsilon u_\ell(1-u_\ell)/m_{1\ell}}{1 + \epsilon(1-u_\ell)/m_{1\ell}} = -\frac{1}{n}\frac{\epsilon\frac{n-1}{n}\frac{1}{m_{1\ell}}}{1 + \epsilon\frac{n-1}{n}\frac{1}{m_{1\ell}}} < 0.\end{aligned} \tag{6.6}$$

Perturbing $m_{i1} \to m_{i1} + \epsilon$ leads to

$$\tilde{u}_\ell - u_\ell = -\frac{\epsilon\, u_1 e_\ell^\top L^\#(e_1 - e_i)}{1 + \epsilon\, e_1^\top L^\#(e_1 - e_i)} = \frac{\epsilon\, u_1 e_\ell^\top L^\#(e_i - e_1)}{1 - \epsilon\, e_1^\top L^\#(e_i - e_1)}.$$

Hence, if $i \neq \ell$,

$$\tilde{u}_\ell - u_\ell = \frac{\epsilon u_1 \bar{e}_{\ell-1}^\top(B^{-1}\bar{e}_{i-1} - \bar{u}\bar{\mathbb{1}}^\top B^{-1}\bar{e}_{i-1})}{1 + \epsilon u_1\bar{\mathbb{1}}^\top B^{-1}\bar{e}_{i-1}} = -\frac{1}{n}\frac{\frac{\epsilon}{n}\frac{1}{m_{1i}}}{1 + \frac{\epsilon}{n}\frac{1}{m_{1i}}} < 0,$$

and if $i = \ell$,

$$\tilde{u}_\ell - u_\ell = \frac{\epsilon u_1 \bar{e}_{\ell-1}^\top(B^{-1}\bar{e}_{\ell-1} - \bar{u}\bar{\mathbb{1}}^\top B^{-1}\bar{e}_{\ell-1})}{1 + \epsilon u_1\bar{\mathbb{1}}^\top B^{-1}\bar{e}_{\ell-1}} = \frac{n-1}{n}\frac{\epsilon\frac{1}{n}\frac{1}{m_{1\ell}}}{1 + \frac{\epsilon}{n}\frac{1}{m_{1\ell}}} > 0.$$

If $i \neq \ell$, then the minimum of $\tilde{u}_\ell - u_\ell$ is achieved at $i = n$. To compare the two different strategies (i.e., $m_{1\ell}$ and m_{n1}), we have the following conclusion: If $m_{1\ell}/m_{1n} < n-1$, the most effective strategy is to increase $m_{1\ell}$; if $m_{1\ell}/m_{1n} > n-1$, the most effective strategy is to increase m_{n1} provided that $n \neq \ell$.

6.2. River with a hot spot. As in subsection 6.1, we introduce a simplifying hypothesis in order to make the analysis more tractable. We assume that $\alpha = 1$ (i.e., $a = b$) and observe that when this is the case, $u = \frac{1}{n}\mathbb{1}$.

We now have the following result.

LEMMA 6.1. *Suppose that $1 \le i < j \le n$. If $\alpha = 1$, then*

$$e_k^\top L^\#(e_j - e_i) = \begin{cases} -\frac{1}{2n}(j-i)(2n-i-j+1), & 1 \le k \le i, \\ (k-j) + \frac{1}{2n}(j-i)(i+j-1), & i < k \le j, \\ \frac{1}{2n}(j-i)(i+j-1), & j < k \le n. \end{cases}$$

Remark 6.1. By Lemma 6.1 and (5.7), it is clear that $\tilde{u}_k - u_k$ is a continuous, piecewise linear function and decreasing in k for $1 \le k \le n$. For $1 \le k \le i$, $\tilde{u}_k - u_k$ is positive and constant in k, while for $j \le k \le n$, $\tilde{u}_k - u_k$ is negative and constant in k.

Assume that we have distinct indices i, j with $1 \le i, j \le n$. By (6.4), to minimize the infection risk, it suffices to minimize $\tilde{u}_\ell - u_\ell$, where ℓ is the hot spot. Perturb $m_{ij} \to m_{ij} + \epsilon$ with $\epsilon > 0$. We have

$$\tilde{u}_\ell - u_\ell = -\frac{\epsilon\, u_j\, e_\ell^\top L^\# (e_j - e_i)}{1 + \epsilon(L^\#_{jj} - L^\#_{ji})} := -u_j g(i,j).$$

When $\alpha = 1$, $u_i = \frac{1}{n}$ for all $1 \le i \le n$ and $\min_{i,j,i\neq j}(\tilde{u}_\ell - u_\ell) = -\frac{1}{n}\max_{i,j,i\neq j} g(i,j)$. Hence, minimizing $\tilde{R}_0 - R_0$ is equivalent to maximizing $g(i,j)$ over distinct i and j with $1 \le i, j \le n$. It turns out that if $\ell \ge \frac{n+1}{2}$, then $\max_{i,j=1,\dots,n,i\neq j} g(i,j) = \frac{\epsilon\ell(\ell-1)}{2n+\epsilon\ell(\ell-1)}$, with the maximum being attained when $i = 1, j = \ell$, while if $\ell \le \frac{n+1}{2}$, then $\max_{i,j=1,\dots,n,i\neq j} g(i,j) = \frac{\epsilon(n+1-\ell)(n-\ell)}{2n+\epsilon(n+1-\ell)(n-\ell)}$, with the maximum being attained when $i = n, j = \ell$. (See supplementary material section (C) for details.) Consequently, the most effective strategy for reducing the risk of infection is to increase $m_{1\ell}$ if the distance between vertices 1 and ℓ is at least as large as the distance between vertices n and ℓ, and to increase $m_{n\ell}$ otherwise.

On the other hand, if $1 \le i < j \le n$ are fixed, by Lemma 6.1, $\min_\ell(\tilde{u}_\ell - u_\ell)$ can be achieved at any $j \le \ell \le n$. Thus, for fixed $i < j$, an increase in m_{ij} will have an equal and greatest effect when the hot spot ℓ is such that $\ell \ge j$.

7. Concluding remarks. Our study, which focuses on disease dynamics, is motivated by modeling directly transmitted diseases [1] and waterborne diseases [17, 44] on patches, under the hypothesis that dispersal between patches is faster than the disease/population dynamics. Our results also shed new light on many spatial ecological studies, for example, the evolution of dispersal in patchy landscapes as studied in [2, 27] in a discrete time model.

Our methods give qualitative and quantitative information about the behavior of the basic reproduction number $\mathcal{R}_0$ as the topology of the network changes and have applications to control strategies for mitigating disease spread among the patches. Our analysis can be thought of as the introduction of connections on the network or of changing the weight of existing connections. In the case that the change in a weight is positive, we have considered optimal strategies for a star and a river network. Our formula (4.2) is valid for all positive perturbations of a network connection, but a negative perturbation must be small for this to remain valid. Optimal strategies can also be formulated for a small negative change, as long as the network remains strongly connected. The effect of breaking this strong connectivity, and thus breaking the network topology, remains to be considered.

In patch models, the monotonicity of $\mathcal{R}_0$ with respect to travel frequency or the diffusion coefficient on a static network has been studied in several papers, for example, [1, 18]; by contrast our results focus on the network topology. The network threshold parameter $\mathcal{R}_0$ governs the invasibility of the disease but not the final size or endemicity of an invading disease. To consider this, it is necessary to use the original dynamical model.

Acknowledgments. The authors thank the American Institute of Mathematics (AIM) for hosting and generously supporting an AIM SQuaRE program focusing on epidemic dynamics of cholera in nonhomogeneous environments, at which this research was initiated and developed. The authors also thank the anonymous reviewers for helpful suggestions.

REFERENCES

[1] L. J. S. Allen, B. M. Bolker, Y. Lou, and A. L. Nevai, *Asymptotic profiles of the steady states for an SIS epidemic patch model*, SIAM J. Appl. Math., 67 (2007), pp. 1283–1309, https://doi.org/10.1137/060672522.

[2] L. Altenberg, *Resolvent positive linear operators exhibit the reduction phenomenon*, Proc. Natl. Acad. Sci. USA, 109 (2012), pp. 3705–3710.

[3] M. Y. Anwar, J. L. Warren, and V. E. Pitzer, *Diarrhea patterns and climate: A spatiotemporal Bayesian hierarchical analysis of diarrheal disease in Afghanistan*, Amer. J. Tropical Med. Hygiene, 101 (2019), pp. 525–533.

[4] M. Baqir, Z. A. Sobani, A. Bhamani, N. S. Bham, S. Abid, J. Farook, and M. A. Beg, *Infectious diseases in the aftermath of monsoon flooding in Pakistan*, Asian Pacific J. Tropical Biomed., 2 (2012), pp. 76–79.

[5] A. Berman and R. J. Plemmons, *Nonnegative Matrices in the Mathematical Sciences*, Classics Appl. Math. 9, SIAM, Philadelphia, 1994, https://doi.org/10.1137/1.9781611971262.

[6] E. Bertuzzo, L. Mari, L. Righetto, M. Gatto, R. Casagrandi, I. Rodriguez-Iturbe, and A. Rinaldo, *Hydroclimatology of dual-peak annual cholera incidence: Insights from a spatially explicit model*, Geophys. Res. Lett., 39 (2012), L05403.

[7] S. L. Campbell and C. D. Meyer, *Generalized Inverses of Linear Transformations,* Classics Appl. Math. 56, SIAM, Philadelphia, 2009, https://doi.org/10.1137/1.9780898719048.

[8] R. S. Cantrell, C. Cosner, M. A. Lewis, and Y. Lou, *Evolution of dispersal in spatial population models with multiple timescales*, J. Math. Biol., 80 (2020), pp. 3–37.

[9] E. J. Carlton, J. N. Eisenberg, J. Goldstick, W. Cevallos, J. Trostle, and K. Levy, *Heavy rainfall events and diarrhea incidence: The role of social and environmental factors*, Amer. J. Epidemiology, 179 (2013), pp. 344–352.

[10] M. Carrel, P. Voss, P. K. Streatfield, M. Yunus, and M. Emch, *Protection from annual flooding is correlated with increased cholera prevalence in Bangladesh: A zero-inflated regression analysis*, Environmental Health, 9 (2010), 13.

[11] S. Chaiken, *A combinatorial proof of the all minors matrix tree theorem*, SIAM J. Alg. Disc. Meth., 3 (1982), pp. 319–329, https://doi.org/10.1137/0603033.

[12] S. Chen, J. Shi, Z. Shuai, and Y. Wu, *Spectral Monotonicity of Perturbed Quasi-positive Matrices with Applications in Population Dynamics*, preprint, https://arxiv.org/abs/1911.02232, 2019.

[13] F. C. Curriero, J. A. Patz, J. B. Rose, and S. Lele, *The association between extreme precipitation and waterborne disease outbreaks in the United States,* 1948–1994, Amer. J. Public Health, 91 (2001), pp. 1194–1199.

[14] E. Deutsch and M. Neumann, *On the first and second order derivatives of the Perron vector*, Linear Algebra Appl., 71 (1985), pp. 57–76.

[15] M. Dhimal, B. Ahrens, and U. Kuch, *Climate change and spatiotemporal distributions of vector-borne diseases in Nepal—a systematic synthesis of literature*, PLOS One, 10 (2015), e0129869.

[16] M. C. Eisenberg, G. Kujbida, A. R. Tuite, D. N. Fisman, and J. H. Tien, *Examining rainfall and cholera dynamics in Haiti using statistical and dynamic modeling approaches*, Epidemics, 5 (2013), pp. 197–207.

[17] M. C. Eisenberg, Z. Shuai, J. H. Tien, and P. van den Driessche, *A cholera model in a patchy environment*, Math. Biosci., 246 (2013), pp. 105–112.

[18] D. Gao, *Travel frequency and infectious diseases*, SIAM J. Appl. Math., 79 (2019), pp. 1581–1606, https://doi.org/10.1137/18M1211957.

[19] D.-Z. Gao and C.-P. Dong, *Fast diffusion inhibits disease outbreaks*, Proc. Amer. Math. Soc., 148 (2020), pp. 1709–1722.

[20] M. Gatto, L. Mari, E. Bertuzzo, R. Casagrandi, L. Righetto, I. Rodriguez-Iturbe, and A. Rinaldo, *Generalized reproduction numbers and the prediction of patterns in waterborne disease*, Proc. Natl. Acad. Sci. USA, 109 (2012), pp. 19703–19708.

[21] A. Gaudiello, *Mathematical Investigation of the Spatial Spread of an Infectious Disease in a Heterogeneous Environment*, Ph.D. thesis, University of Central Florida, 2019.

[22] S. Gourley, R. Liu, and J. Wu, *Spatiotemporal patterns of disease spread: Interaction of physiological structure, spatial movements, disease progression and human intervention*, in Structured Population Models in Biology and Epidemiology, Math. Biosci. Subser. 1936, P. Magal and S. Ruan, eds., Springer-Verlag, Berlin, 2008, pp. 165–208.

[23] M. Hashizume, B. Armstrong, S. Hajat, Y. Wagatsuma, A. S. Faruque, T. Hayashi, and D. A. Sack, *The effect of rainfall on the incidence of cholera in Bangladesh*, Epidemiology, 19 (2008), pp. 103–110.

[24] R. A. Horn and C. R. Johnson, *Matrix Analysis*, Cambridge University Press, Cambridge, 2013.

[25] S. Karlin, *Classifications of selection—migration structures and conditions for a protected polymorphism*, in Evolutionary Biology, Vol. 14, Plenum Press, New York, 1982, pp. 61–204.

[26] R. B. Kaul, M. V. Evans, C. C. Murdock, and J. M. Drake, *Spatio-temporal spillover risk of yellow fever in Brazil*, Parasites & Vectors, 11 (2018), 488.

[27] S. Kirkland, C.-K. Li, and S. J. Schreiber, *On the evolution of dispersal in patchy landscapes*, SIAM J. Appl. Math., 66 (2006), pp. 1366–1382, https://doi.org/10.1137/050628933.

[28] S. J. Kirkland and M. Neumann, *Group Inverses of M–Matrices and Their Applications*, CRC Press, Boca Raton, FL, 2013.

[29] K. Levy, S. M. Smith, and E. J. Carlton, *Climate change impacts on waterborne diseases: Moving toward designing interventions*, Current Environmental Health Reports, 5 (2018), pp. 272–282.

[30] K. Levy, A. P. Woster, R. S. Goldstein, and E. J. Carlton, *Untangling the impacts of climate change on waterborne diseases: A systematic review of relationships between diarrheal diseases and temperature, rainfall, flooding, and drought*, Environmental Sci. Tech., 50 (2016), pp. 4905–4922.

[31] A. López-Quílez, *Spatio-temporal analysis of infectious diseases*, Int. J. Environ. Res. Public Health, 16 (2019), 669.

[32] M. Á. Luque Fernández, A. Bauernfeind, J. D. Jiménez, C. L. Gil, N. E. Omeiri, and D. H. Guibert, *Influence of temperature and rainfall on the evolution of cholera epidemics in Lusaka, Zambia,* 2003–2006*: Analysis of a time series*, Trans. R. Soc. Tropical Med. Hygiene, 103 (2009), pp. 137–143.

[33] L. Mari, R. Casagrandi, E. Bertuzzo, A. Rinaldo, and M. Gatto, *Conditions for transient epidemics of waterborne disease in spatially explicit systems*, R. Soc. Open Sci., 6 (2019), 181517.

[34] C. D. Meyer, Jr., *The condition of a finite Markov chain and perturbation bounds for the limiting probabilities*, SIAM J. Alg. Disc. Meth., 1 (1980), pp. 273–283, https://doi.org/10.1137/0601031.

[35] C. D. Meyer, *Matrix Analysis and Applied Linear Algebra*, SIAM, 2000.

[36] J. W. Moon, *Counting Labelled Trees*, Canadian Mathematical Congress, Montreal, Canada, 1970.

[37] M. H. Myer and J. M. Johnston, *Spatiotemporal Bayesian modeling of West Nile virus: Identifying risk of infection in mosquitoes with local-scale predictors*, Sci. Total Environment, 650 (2019), pp. 2818–2829.

[38] J. Okpasuo, F. Okafor, and I. Aguzie, *Effects of household drinking water choices, knowledge, practices and spatio-temporal trend on the prevalence of waterborne diseases in Enugu Urban, Nigeria*, Int. J. Infectious Diseases, 73 (2018), pp. 225–226.

[39] M. G. Rosa-Freitas, N. A. Honório, C. T. Codeço, G. L. Werneck, and N. Degallier, *Spatial studies on vector-transmitted diseases and vectors*, J. Tropical Med., 2012 (2012), 573965.

[40] G. Rossi, S. Karki, R. L. Smith, W. M. Brown, and M. O. Ruiz, *The spread of mosquito-borne viruses in modern times: A spatio-temporal analysis of dengue and chikungunya*, Spatial and Spatio-temporal Epidemiology, 26 (2018), pp. 113–125.

[41] M. S. Sarfraz, N. K. Tripathi, T. Tipdecho, T. Thongbu, P. Kerdthong, and M. Souris, *Analyzing the spatio-temporal relationship between dengue vector larval density and land-use using factor analysis and spatial ring mapping*, BMC Public Health, 12 (2012), 853.

[42] W. Sun, L. Xue, and X. Xie, *Spatial-temporal distribution of dengue and climate characteristics for two clusters in Sri Lanka from* 2012 *to* 2016, Sci. Rep., 7 (2017), 12884.

[43] A. J. Tatem, D. J. Rogers, and S. I. Hay, *Global transport networks and infectious disease spread*, Adv. Parasitology, 62 (2006), pp. 293–343.

[44] J. H. Tien, Z. Shuai, M. C. Eisenberg, and P. van den Driessche, *Disease invasion on community networks with environmental pathogen movement*, J. Math. Biol., 70 (2015), pp. 1065–1092.

[45] A. Venkat, T. M. A. Falconi, M. Cruz, M. A. Hartwick, S. Anandan, N. Kumar, H. Ward, B. Veeraraghavan, and E. N. Naumova, *Spatiotemporal patterns of cholera hospitalization in Vellore, India*, Int. J. Environ. Res. Public Health, 16 (2019), 4257.

[46] L. S. Waldron, B. Dimeski, P. J. Beggs, B. C. Ferrari, and M. L. Power, *Molecular epidemiology, spatiotemporal analysis, and ecology of sporadic human cryptosporidiosis in Australia*, Appl. Environ. Microbiol., 77 (2011), pp. 7757–7765.

[47] L. A. Waller, B. J. Goodwin, M. L. Wilson, R. S. Ostfeld, S. L. Marshall, and E. B. Hayes, *Spatio-temporal patterns in county-level incidence and reporting of Lyme disease in the northeastern United States,* 1990–2000, Environ. Ecol. Stat., 14 (2007), 83.

SUPPLEMENTARY MATERIALS: IMPACT OF VARYING COMMUNITY NETWORKS ON DISEASE INVASION*

STEPHEN KIRKLAND†, ZHISHENG SHUAI‡, P. VAN DEN DRIESSCHE§, AND XUEYING WANG¶

(A) A version of the multi-patch cholera model in [SM2, SM3], simplified by ignoring host movement, takes the following form:

$$\begin{aligned}
\frac{dS_i}{dt} &= A_i - g_i(S_i, W_i) - d_i S_i,\\
\frac{dI_i}{dt} &= g_i(S_i, W_i) - (d_i + \alpha_i + \gamma_i) I_i,\\
\frac{dR_i}{dt} &= \gamma_i I_i - d_i R_i,\\
\frac{dW_i}{dt} &= r_i I_i - \delta_i W_i + \sum_{j=1}^{n} \left(m_{ij} W_j - m_{ji} W_i\right),
\end{aligned}$$

with variables and parameters summarized in the following list:

S_i, I_i, R_i	:	susceptible, infectious and recovered host population in patch i
W_i	:	the concentration of cholera bacteria in the water source in patch i
$A_i > 0$	:	constant recruitment into patch i
$d_i > 0$	:	natural death rate in patch i
$\alpha_i \geq 0$	:	cholera induced death rate in patch i
$\gamma_i > 0$	:	recovery rate of infectious individuals in patch i
$r_i \geq 0$	:	pathogen shedding rate in patch i
$\delta_i > 0$	:	removal rate of pathogen in patch i
$m_{ij} \geq 0$	:	travel rate of pathogen from patch j to patch i
$g_i(S_i, W_i) \geq 0$	:	incidence function for cholera transmission in patch i

Linearization at the disease-free equilibrium $(\frac{A_1}{d_1}, 0, 0, 0, \cdots, \frac{A_n}{d_n}, 0, 0, 0)$ and reducing to the disease compartments (i.e., I_i and W_i) yield the Jacobian matrix $J = F - V$ with $F = \begin{pmatrix} 0 & D_q \\ 0 & 0 \end{pmatrix}$ and $V = \begin{pmatrix} G_I & 0 \\ -D_r & G_W \end{pmatrix}$. Here $D_q = \text{diag}\{q_i\} := \text{diag}\{\frac{\partial g_i}{\partial W_i}(\frac{A_i}{d_i}, 0)\}$, $G_W = \text{diag}\{\delta_i\} + L$ with L being the Laplacian matrix as defined in (2.1), $D_r = \text{diag}\{r_i\}$ and $G_I = \text{diag}\{\mu_i\} := \text{diag}\{d_i + \alpha_i + \gamma_i\}$. Thus the basic reproduction number $\mathcal{R}_0$ is defined as the spectral radius of the next generation matrix FV^{-1}; that is, $\mathcal{R}_0 = \rho(FV^{-1}) = \rho(D_q G_W^{-1} D_r G_I^{-1})$.

For directly transmitted disease models such as the SIS model in [SM1], the basic reproduction number $\mathcal{R}_0 = \rho(\text{diag}\{\beta_i\}(\text{diag}\{\eta_i\} + d_I L)^{-1})$, where β_i is the disease transmission coefficient for the standard incidence, η_i is the rate of infectious

*Supplementary material for SIAP MS#M132876.
https://doi.org/10.1137/20M1328762

†Department of Mathematics, University of Manitoba, Winnipeg, MB, R3T 2N2, Canada (Stephen.Kirkland@umanitoba.ca).

‡Department of Mathematics, University of Central Florida, Orlando, FL 32816 USA (shuai@ucf.edu).

§Department of Mathematics and Statistics, University of Victoria, Victoria, BC, V8W 2Y2, Canada (pvdd@math.uvic.ca).

¶Department of Mathematics and Statistics, Washington State University, Pullman, WA 99164-3113 USA (xueying@math.wsu.edu).

individuals becoming susceptible again, and d_I represents the scale of movement rate of infectious individuals.

(B) Suppose that $\hat{L}$ is given by (5.5). We claim that it suffices to consider the case that $a \geq b$. To see the claim, first note that $\hat{L} = P\overline{L}P^\top$, where

$$\overline{L} = \begin{pmatrix} b & -a & 0 & \cdots & 0 & 0 \\ -b & a+b & -a & \cdots & 0 & 0 \\ 0 & -b & a+b & \cdots & 0 & 0 \\ \vdots & \vdots & & & & \\ 0 & 0 & 0 & \cdots & a+b & -a \\ 0 & 0 & 0 & \cdots & -b & a \end{pmatrix}$$

and P is the $n \times n$ "back diagonal" permutation matrix such that $p_{j\ n+1-j} = 1, j = 1, \ldots, n$. If it happens that $a < b$, we then work with $\overline{L}$ instead of $\hat{L}$.

(C) Here we derive the expression for $\max_{i,j=1,\ldots,n,i\neq j} g(i,j)$ given at the end of section 6.2. We begin by supposing that $1 \leq i < j \leq n$. If $1 \leq \ell \leq i$, then by Lemma 6.1, $g(i,j) = \dfrac{\epsilon\left[-\frac{1}{2n}(j-i)(2n-i-j+1)\right]}{1+\epsilon\frac{1}{2n}(j-i)(i+j-1)}$. Hence, for $1 \leq \ell \leq i$, the maximum value of $g(i,j)$ is achieved when $i = n-1$ and $j = n$, with $g(n-1,n) = -\dfrac{\epsilon}{n+\epsilon(n-1)}$.

If $j \leq \ell \leq n$, then by Lemma 6.1, $g(i,j) = \dfrac{\epsilon\left[\frac{1}{2n}(j-i)(i+j-1)\right]}{1+\epsilon\frac{1}{2n}(j-i)(i+j-1)}$. Thus when $j \leq \ell \leq n$, the maximum value of $g(i,j)$ is achieved when $j = \ell$ and $i = 1$, with $g(1,\ell) = \dfrac{\epsilon\ell(\ell-1)}{2n+\epsilon\ell(\ell-1)}$.

For the intermediate case where $i < \ell \leq j$, using Lemma 6.1, we have

$$g(i,j) = \frac{\epsilon\left[(\ell-j)+\frac{1}{2n}(j-i)(i+j-1)\right]}{1+\epsilon\frac{1}{2n}(j-i)(i+j-1)} \leq \frac{\epsilon\left[\frac{1}{2n}(j-i)(i+j-1)\right]}{1+\epsilon\frac{1}{2n}(j-i)(i+j-1)}.$$

From the considerations above, it follows that for $1 \leq i < j \leq n$, the maximum value of $g(i,j)$ is $\dfrac{\epsilon\ell(\ell-1)}{2n+\epsilon\ell(\ell-1)}$, which is achieved when $j = \ell$ and $i = 1$.

Next, consider the case that $1 \leq j < i \leq n$. A parallel argument (which proceeds by considering the indices $n+1-j, n+1-i$ and $n+1-\ell$) shows that $\max_{1\leq j<i\leq n} g(i,j) = \dfrac{\epsilon(n+1-\ell)(n-\ell)}{2n+\epsilon(n+1-\ell)(n-\ell)}$. We deduce that

$$\max_{i,j=1,\ldots,n,i\neq j} g(i,j) = \max\left\{\frac{\epsilon\ell(\ell-1)}{2n+\epsilon\ell(\ell-1)}, \frac{\epsilon(n+1-\ell)(n-\ell)}{2n+\epsilon(n+1-\ell)(n-\ell)}\right\}.$$

More specifically, if $\ell \geq \dfrac{n+1}{2}$, then $\max_{i,j=1,\ldots,n,i\neq j} g(i,j) = \dfrac{\epsilon\ell(\ell-1)}{2n+\epsilon\ell(\ell-1)}$, and the maximum is attained for $i = 1, j = \ell$; on the other hand, if $\ell \geq \dfrac{n+1}{2}$, then $\max_{i,j=1,\ldots,n,i\neq j} g(i,j) = \dfrac{\epsilon(n+1-\ell)(n-\ell)}{2n+\epsilon(n+1-\ell)(n-\ell)}$, and the maximum is attained for $i = n, j = \ell$.

REFERENCES

[SM1] L. J. S. Allen, B. M. Bolker, Y. Lou, and A. L. Nevai, *Asymptotic profiles of the steady states for an SIS epidemic patch model*, SIAM J. Appl. Math., 67 (2007), pp. 1283–1309.

[SM2] M. C. Eisenberg, Z. Shuai, J. H. Tien, and P. van den Driessche, *A cholera model in a patchy environment*, Math. Biosci., 246 (2013), pp. 105–112.

[SM3] J. H. Tien, Z. Shuai, M. C. Eisenberg, and P. van den Driessche, *Disease invasion on community networks with environmental pathogen movement*, J. Math. Biol., 70 (2015), pp. 1065–1092.